

International Atomic Energy Agency

INDC(CCP)-30/U

INDC

INTERNATIONAL NUCLEAR DATA COMMITTEE

NUCLEAR PHYSICS RESEARCH IN THE USSR

(Collected Abstracts)

No.12

Translated by the IAEA
December 1972

IAEA NUCLEAR DATA SECTION, KÄRNTNER RING 11, A-1010 VIENNA

USSR STATE COMMITTEE ON THE UTILIZATION OF ATOMIC ENERGY
NUCLEAR DATA INFORMATION CENTRE

NUCLEAR PHYSICS RESEARCH IN THE USSR

(Collected Abstracts)
No.12

English translation of an original in Russian published by
Atomizdat, 1971

EDITORIAL BOARD

V.A. KUZNETSOV (Chief Scientific Editor), L.N. USACHEV (Deputy
Chief Scientific Editor), Yu.V. ADAMCHUK, V.N. ANDREEV,
G.Z. BORUKHOVICH, V.P. ZOMMER, I.A. KORZH, V.A. NAUMOV,
A.I. OBUCHOV, Yu.P. POPOV, D.A. KARDASHEV (Editor-in-Chief).

INSTITUTE OF PHYSICS AND POWER ENGINEERING

FISSION CROSS-SECTION OF ^{249}Cf FOR THERMAL AND FAST NEUTRONS

B.I. Fursov, Kh.D. Androsenko, V.I. Ivanov, V.G. Nesterov
G.N. Smirenkin, L.V. Chistyakov, V.M. Shubko

(Submitted to Atomnaja Energija)

The authors describe the results of measurements of the fission cross-section and angular anisotropy of fission fragments of ^{249}Cf for thermal and fast neutrons. The measurements involving thermal neutrons were carried out in the thermal column of the BR-5 reactor. The fast neutron source was an electrostatic generator. The measurements were performed for neutron energies of 500, 750, 850, 1450, 4000, 4500 and 5020 keV. Results are shown in Table 1.

Table 1

	E_n MeV	ΔE_n MeV	$\frac{\sigma_f(Cf^{249})}{\sigma_f(Pu^{239})}$	$\Delta \left(\frac{\sigma_f(Cf^{249})}{\sigma_f(Pu^{239})} \right)^*$	$\sigma_f(Pu^{239})$ barn	$\sigma_f(Cf^{249})$ barn	$\Delta \sigma_f(Cf^{249})$ barn	$\frac{\sigma_f(0^\circ)}{\sigma_f(90^\circ)}$	$\Delta \left(\frac{\sigma_f(0^\circ)}{\sigma_f(90^\circ)} \right)$
1.		-	2,150	$\pm 0,050$	790	1700	± 40	-	-
2.	0,500	$\pm 0,090$	0,997	$\pm 0,030$	1,59	1,58	$\pm 0,05$	0,102	$\pm 0,050$
3.	0,750	$\pm 0,080$	0,876	$\pm 0,027$	1,64	1,44	$\pm 0,05$	0,030	$\pm 0,080$
4.	0,850	$\pm 0,075$	0,810	$\pm 0,025$	1,68	1,36	$\pm 0,06$	0,133	$\pm 0,060$
5.	1,450	$\pm 0,070$	0,866	$\pm 0,030$	1,93	1,67	$\pm 0,06$	0,137	$\pm 0,060$
6.	4,000	$\pm 0,100$	1,072	$\pm 0,042$	1,82	1,95	$\pm 0,08$	0,134	$\pm 0,080$
7.	4,500	$\pm 0,100$	1,120	$\pm 0,039$	1,78	1,99	$\pm 0,07$	0,209	$\pm 0,060$
8.	5,020	$\pm 0,100$	1,135	$\pm 0,034$	1,76	2,00	$\pm 0,06$	0,158	$\pm 0,050$

* Reference values for ^{239}Pu fission cross-sections were taken from Ref. [3] for thermal neutrons and from Ref. [4] for fast neutrons.

RATIO OF NEUTRON RADIATIVE CAPTURE AND FISSION CROSS-SECTIONS
FOR PLUTONIUM-239 IN THE ENERGY RANGE BELOW ~50 keV

A.A. Bergman, Yu.Ya. Stavissky, V.B. Chelnokov,
A.E. Samsonov, V.A. Tolstikov, A.N. Medvedev

The authors present the results of measurements of the parameter $\alpha(E)$ (the ratio of neutron radiative capture and fission cross-sections) for plutonium-239 which were performed on a spectrometer using the slowing-down time in lead.

The main feature of the method is that the sample and the detector are located in an isotropic neutron field, which does not vary due to neutron scattering by nuclei of the sample and the material of the detector. The low gamma background level of the spectrometer makes it possible to record the prompt gamma rays from radiative capture and fission with a gas proportional counter, on which the gamma ray recording efficiency is proportional to their energy. Measurements of the fission effect were performed with an ionization fission chamber.

The relative energy dependence of the cross-sections was normalized using a well-thermalized neutron spectrum obtained in a graphite prism placed close to the main prism of the lead moderator.

The results of the measurements, averaged over the ranges corresponding to the energy resolution of the spectrometer, are given in Table 1.

Table 1

Averaged values for neutron fission and radiative-capture cross-sections and for the parameter $\alpha(E)$ for plutonium-239

Energy range, eV	$\langle \bar{\sigma}_f(E) \rangle$ barn	$\langle \alpha(E) \rangle$	$\langle \bar{\sigma}_c(E) \rangle$, barn
60000 - 20000	1,43 ± 0,11	0,39 ± 0,14	0,56 ± 0,20
20000 - 9000	1,61 ± 0,11	0,70 ± 0,15	1,12 ± 0,25
9000 - 4000	2,02 ± 0,11	0,89 ± 0,16	1,80 ± 0,34
4000 - 2000	2,66 ± 0,14	0,99 ± 0,16	2,63 ± 0,45
2000 - 1000	4,06 ± 0,22	1,12 ± 0,16	4,6 ± 0,7
1000 - 700	5,80 ± 0,30	1,06 ± 0,15	6,1 ± 0,9
700 - 400	8,21 ± 0,45	0,95 ± 0,14	7,8 ± 1,2
400 - 200	12,8 ± 0,7	0,89 ± 0,13	11,4 ± 1,8
200 - 100	18,5 ± 0,8	0,71 ± 0,12	13,1 ± 2,5

METHOD OF MEASURING THE RADIATIVE CAPTURE TO
FISSION CROSS-SECTION RATIO

V.G. Dvukhsherstnov, Yu.A. Kazansky,
E.A. Plaksin, V.M. Furmanov

A method is described for measuring the radiative capture to fission cross-section ratio α , based on the use of a single-crystal scintillation spectrometer with separate channels for recording neutrons and gamma rays. The authors discuss the correction factors involved and the accuracy of measuring α by this method. The value of alpha was measured for uranium-235 and plutonium-239 in the "scandium" and "iron" beams of the reactor at Obninsk Nuclear Power Station. Table 1 shows the results of the measurements for neutrons with energies of 2 ± 0.35 and 24.5 ± 1.0 keV (the results for $E_0 = 24.5$ keV are provisional).

Table 1

E_0 , keV	$\alpha (E_0)$ for ^{235}U	$\alpha (E_0)$ for ^{239}Pu
2 ± 0.35	0.49 ± 0.04	1.35 ± 0.09
24.5 ± 1.0	0.43 ± 0.14	0.30 ± 0.09

ABSOLUTE MEASUREMENTS OF α FOR ^{235}U AND ^{239}Pu
IN THE 10 keV-1 MeV NEUTRON ENERGY REGION

V.N. Kononov, E.D. Poletaev, Yu.S. Prokopets,
A.A. Metlev, Yu.Ya. Stavitsky

The radiative capture to fission cross-section ratios for ^{235}U and ^{239}Pu were measured on a pulsed Van de Graaff accelerator using the time-of-flight method for the 10 keV-1 MeV neutron energy range. The capture and fission events were recorded with a liquid scintillation detector having a volume of 400 l. The capture and fission events were identified from the recording of the fission neutrons after they had been slowed down and absorbed in cadmium. In the 10-80 keV neutron energy range the experiment was performed on a continuous neutron spectrum from the reaction $^7\text{Li}(p,n)^7\text{Be}$ and the neutron energy was measured by the time-of-flight method. At higher energies the experiment was performed with monoenergetic neutrons. An absolute method of measuring α was used.

The basic α values obtained for ^{235}U and ^{239}Pu are shown in Tables 1 and 2. The tables also show the root-mean-square error of the energy dependence of α (including only the statistical error) and the total root-mean-square error in the value of α . The samples used for the experiments were metallic ^{239}Pu with a thickness of 2.9×10^{-21} nuclei/cm² and $^{235}\text{U}_3\text{O}_8$ with a thickness of 4.1×10^{-21} ^{235}U nuclei/cm².

Table 1

Value of α for ^{235}U , obtained in the present study

E_n , keV	α	$\sigma\alpha$ rel. to trend	$\sigma\alpha$ total error
12,4 \pm 0,7	0,549	0,043	0,057
13,4 \pm 0,8	0,476	0,061	0,069
14,3 \pm 0,8	0,457	0,040	0,051
15,4 \pm 0,9	0,531	0,032	0,048
15,9 \pm 1,0	0,452	0,030	0,043
16,4 \pm 1,0	0,424	0,031	0,042
16,9 \pm 1,1	0,365	0,032	0,041
17,4 \pm 1,1	0,350	0,026	0,036
17,9 \pm 1,2	0,394	0,033	0,043
18,5 \pm 1,2	0,398	0,024	0,036
19,1 \pm 1,3	0,370	0,020	0,033
19,8 \pm 1,4	0,338	0,029	0,038
20,4 \pm 1,4	0,317	0,024	0,033
21,1 \pm 1,5	0,307	0,020	0,030
21,9 \pm 1,6	0,337	0,034	0,042
22,7 \pm 1,7	0,339	0,021	0,031
23,5 \pm 1,8	0,344	0,021	0,032
24,3 \pm 1,9	0,336	0,013	0,030
25,3 \pm 2,0	0,283	0,017	0,026
26,2 \pm 2,0	0,268	0,019	0,027
27,3 \pm 2,2	0,292	0,014	0,025
28,4 \pm 2,4	0,312	0,016	0,027
29,5 \pm 2,5	0,333	0,017	0,029
30,7 \pm 2,7	0,346	0,019	0,031
32,1 \pm 2,8	0,350	0,019	0,031
33,4 \pm 3,0	0,342	0,018	0,030
34,9 \pm 3,2	0,350	0,017	0,030
36,5 \pm 3,4	0,340	0,020	0,031
38,2 \pm 3,7	0,346	0,019	0,031
40,0 \pm 3,9	0,332	0,019	0,030
42,0 \pm 4,2	0,335	0,019	0,030
44,1 \pm 4,6	0,308	0,011	0,025
46,3 \pm 4,9	0,307	0,016	0,027

Table 1 (continued)

E_n , keV	α	σ_α rel. to trend	σ_α total error
48,8 ± 5,3	0,300	0,017	0,027
51,4 ± 5,7	0,285	0,016	0,026
54,3 ± 6,2	0,288	0,018	0,027
57,4 ± 6,8	0,277	0,015	0,025
60,8 ± 7,4	0,292	0,013	0,025
90 ± 15	0,307	0,020	0,030
135 ± 25	0,247	0,015	0,024
185 ± 15	0,218	0,010	0,019
300 ± 10	0,181	0,011	0,018
400 ± 10	0,183	0,010	0,018
500 ± 10	0,150	0,006	0,014
750 ± 30	0,127	0,011	0,012
900 ± 30	0,101	0,010	0,014
1100 ± 30	0,077	0,009	0,013

Table 2

Value of α for ^{239}Pu , obtained in the present study

E_n , keV	α	σ_α rel. to trend	σ_α total error
9,4 ± 0,5	0,502	0,079	0,085
10,4 ± 0,5	0,508	0,058	0,067
11,3 ± 0,6	0,572	0,041	0,055
12,2 ± 0,7	0,517	0,068	0,076
13,1 ± 0,7	0,538	0,077	0,084
14,2 ± 0,8	0,478	0,037	0,048
15,2 ± 0,9	0,418	0,054	0,061
15,9 ± 1,0	0,366	0,038	0,045
16,4 ± 1,0	0,342	0,042	0,049
16,8 ± 1,1	0,331	0,032	0,040
17,3 ± 1,1	0,325	0,028	0,037
17,9 ± 1,2	0,329	0,030	0,038
18,4 ± 1,2	0,316	0,026	0,035
19,2 ± 1,3	0,328	0,031	0,039

Table 2 (continued)

E_n , keV	χ	σ_a rel. to trend	σ_a total error
19,6 ± 1,4	0,340	0,025	0,034
20,3 ± 1,4	0,352	0,032	0,040
20,9 ± 1,5	0,346	0,021	0,032
21,6 ± 1,6	0,369	0,018	0,030
22,4 ± 1,7	0,348	0,015	0,029
23,2 ± 1,7	0,346	0,022	0,033
24,0 ± 1,8	0,320	0,018	0,029
24,8 ± 1,9	0,316	0,015	0,027
25,8 ± 2,0	0,330	0,022	0,032
26,7 ± 2,2	0,302	0,017	0,027
27,8 ± 2,3	0,293	0,015	0,026
28,8 ± 2,4	0,282	0,021	0,030
30,0 ± 2,6	0,247	0,011	0,022
31,2 ± 2,7	0,258	0,011	0,022
32,5 ± 2,9	0,272	0,012	0,024
33,9 ± 3,1	0,286	0,016	0,026
35,3 ± 3,3	0,260	0,015	0,025
36,9 ± 3,5	0,260	0,009	0,022
38,6 ± 3,4	0,243	0,011	0,022
40,4 ± 4,0	0,247	0,014	0,024
42,3 ± 4,3	0,240	0,010	0,021
44,3 ± 4,6	0,225	0,007	0,020
46,5 ± 4,9	0,213	0,006	0,019
48,9 ± 5,3	0,207	0,009	0,020
51,4 ± 5,7	0,193	0,007	0,018
54,2 ± 6,2	0,176	0,008	0,018
57,2 ± 6,7	0,174	0,007	0,018
60,4 ± 7,3	0,170	0,005	0,017
64 ± 8,0	0,172	0,006	0,017
110 ± 20	0,149	0,007	0,015
150 ± 25	0,115	0,010	0,016
185 ± 15	0,090	0,009	0,015
300 ± 10	0,103	0,012	0,018
400 ± 10	0,075	0,009	0,015
500 ± 10	0,082	0,010	0,015
750 ± 30	0,071	0,009	0,015
900 ± 30	0,032	0,006	0,012
100 ± 30	0,008	0,013	0,017

NEUTRON YIELD AND KINETIC ENERGY OF FRAGMENTS IN
THERMAL FISSION OF ^{249}Cf

K.E. Volodin, V.G. Nesterov, B. Nurpeisov, G.N. Smirenkin,
Yu.M. Turchin, V.N. Kosyakov, L.V. Chistyakov, I.K. Shvetsov,
V.M. Shubko, L.N. Mezentsev, V.N. Okolovich

(Submitted to *Jadernaja Fizika*)

Measurements were made of the mean number of prompt neutrons ($\bar{\nu} = 4.06 \pm 0.04$) and the mean kinetic energy of the fragments ($\bar{E}_k = 187.3 \pm 1.5$ MeV) for thermal neutron fission of ^{249}Cf . The dependence of $\bar{\nu}$ and \bar{E}_k on the nucleonic composition of the fissioning nucleus is discussed.

THE GENETIC CONNECTION BETWEEN DELAYED NEUTRON
RADIATION AND THE FISSION PROCESS

B.P. Maksyutenko

The genetic connection between delayed neutron radiation and the fission process is considered. A method is developed, by which it is possible, on the basis of data for the relative delayed neutron yield from the thermal fission of ^{235}U , to calculate quite accurately the number of prompt fission neutrons and the dispersion of the distribution of the number of prompt fission neutrons. It is shown that this method can be employed for calculating the same values for fast fission.

After analysing the relationships of the fission product charge and the cumulative yields, the author examines the correlation between the number of prompt fission neutrons emitted and fragment mass. The width of the excitation energy distribution during fission is found. The following results are obtained:

$$\bar{\nu} = 2.55 \text{ (mean number of prompt fission neutrons produced in thermal fission of } ^{235}\text{U)};$$

$$\text{Dispersion: } \sigma_{\nu} = 1.30.$$

CROSS-SECTIONS FOR THE FORMATION OF GAMMA RAYS DURING
INELASTIC SCATTERING OF NEUTRONS IN THE SPECTRUM
OF A URANIUM-WATER REACTOR

A.T. Bakov, V.G. Dvukhshestnov, Yu.A. Kazansky

The mean gamma ray yield cross-sections (separate lines or groups of unresolved lines) were measured in the neutron spectrum of a uranium-water reactor $\varphi(E_n)$ for Na, Al, Ti, V, Mn, Fe, Ni, Cu, Zn, Zr, W, Pl, Bi and ^{238}U , using a single-crystal scintillation gamma ray spectrometer with neutron discrimination according to de-excitation time. Since the cross-sections $\langle \sigma_{\gamma i} \rangle$ depend essentially on the type of neutron spectrum, the authors propose a more conservative system for calculating the quantity of gamma rays from inelastic scattering in a neutron spectrum different from that used in this experiment, i.e. a system involving a quantity which is less dependent on the shape of the neutron spectrum:

$$\langle \xi_{\gamma i} \rangle = \frac{\int_{E_{\text{lim}}}^{\infty} \varphi(E_n) \sigma_{\gamma i}(E_n) dE_n}{\int_{\infty}^{\infty} \varphi(E_n) \sigma_{\text{in}}(E_n) dE_n}$$

where E_{lim} is the neutron energy, at which the emission of gamma rays of energy E_{γ} is possible in inelastic scattering of neutrons of energy $E_n \geq E_{\text{lim}}$.

CORRECTION FOR MULTIPLE NEUTRON SCATTERING IN "THIN" SPECIMENS

V.S. Shorin

(Preprint, Institute of Physics and Power Engineering)

The effects of multiple neutron scattering are considered on the basis of a one-velocity approximation of "initial collisions". The analysis concerns cylindrical samples with a thickness of $\Sigma t \leq 0.25$ subjected to wide plane-parallel neutron flux.

ELECTRONIC EQUIPMENT FOR AN EXPERIMENT TO MEASURE THE RADIATIVE
CAPTURE TO FISSION CROSS-SECTION RATIO IN THE FAST
NEUTRON REGION

E.D. Poletaev, V.N. Kononov, M.V. Bokhovko

The authors describe the electronic equipment used in an experiment to make absolute measurements of the radiative capture to fission cross-section ratios for ^{239}Pu and ^{235}U in the 10 keV-1 MeV energy region on a pulsed Van de Graaff accelerator. The equipment provides a means of identifying capture and fission events and measuring neutron energy from the time-of-flight.

I.V. KURCHATOV ATOMIC ENERGY INSTITUTE

THE ENERGY DEPENDENCE OF $\bar{\nu}$ FOR THE FISSION
OF ^{238}U BY FAST NEUTRONS

(Paper presented at the Conference on Neutron Physics, Kiev, 1971)

M.V. Savin, Yu.A. Khokhlov, I.N. Paramonova, V.A. Chirkin

The results are given of measurements of $\bar{\nu}$ in fission of ^{238}U by neutrons with energies of 1.3-7 MeV. The measurements were performed in a linear electron accelerator by the time-of-flight method (resolution 1 nsec/m), use having been made of a liquid scintillation detector. The energy dependence of $\bar{\nu}(E)_n$ measured in the experiment is described by a broken line with two gradients of $\frac{d\bar{\nu}}{dE_n} = 0.10$ for $E_n < 3$ MeV and $\frac{d\bar{\nu}}{dE_n} = 0.18$ for $E_n > 3$ MeV. The accuracy of determining absolute values of $\bar{\nu}$ is 1.5-3% in this particular energy range.

Table 1

The average number of prompt neutrons in fission of ^{238}U

E_n /MeV/	$\bar{\nu}$	E_n /MeV/	$\bar{\nu}$	E_n /MeV/	$\bar{\nu}$
1,27	2,503 ± 0,055	2,18	2,610 ± 0,039	3,80	2,680 ± 0,057
1,30	2,498 ± 0,052	2,24	2,618 ± 0,042	3,94	2,886 ± 0,058
1,33	2,544 ± 0,051	2,31	2,653 ± 0,042	4,09	2,911 ± 0,061
1,35	2,575 ± 0,049	2,37	2,679 ± 0,043	4,24	2,876 ± 0,058
1,42	2,591 ± 0,046	2,44	2,708 ± 0,043	4,50	2,981 ± 0,057
1,45	2,591 ± 0,046	2,51	2,652 ± 0,042	4,66	3,023 ± 0,057
1,48	2,518 ± 0,045	2,59	2,609 ± 0,044	5,39	3,095 ± 0,080
1,51	2,470 ± 0,044	2,66	2,630 ± 0,045	5,62	3,186 ± 0,092
1,55	2,467 ± 0,042	2,74	2,613 ± 0,044	5,27	3,184 ± 0,092
1,58	2,576 ± 0,044	2,83	2,661 ± 0,045		
1,62	2,577 ± 0,041	2,92	2,644 ± 0,047		
1,70	2,639 ± 0,042	3,11	2,689 ± 0,048		

Table 1 (continued)

E_n /MeV/	$\bar{\nu}$	E_n /MeV/	$\bar{\nu}$
1,78	$2,552 \pm 0,041$	3,21	$2,721 \pm 0,049$
1,82	$2,589 \pm 0,041$	3,32	$2,721 \pm 0,049$
1,87	$2,586 \pm 0,041$	3,43	$2,812 \pm 0,053$
1,92	$2,543 \pm 0,041$	3,55	$2,778 \pm 0,053$
1,97	$2,621 \pm 0,039$	3,68	$2,819 \pm 0,056$
2,02	$2,591 \pm 0,039$		
2,07	$2,587 \pm 0,041$		
2,13	$2,612 \pm 0,039$		

MEASUREMENT OF THE CAPTURE TO FISSION
CROSS-SECTION RATIO FOR ^{235}U

P.E. Vorotnikov, V.A. Vukolov, E.A. Koltypin,
Yu.D. Molchanov, G.B. Yankov

The development of fast reactors has made it necessary to provide more accurate values of $\alpha = \sigma_{ne} / \sigma_{nf}$, especially in the neutron energy range from a few keV to 100 keV. It was desirable to use a different measuring technique from that used earlier by other authors [1-6], in order to avoid the systematic errors produced.

In our work the α -values for ^{235}U were measured by a direct method in the 5-50 keV and 130 keV neutron energy ranges.

Experimental method

The measurements were performed in an electrostatic accelerator under pulsed operating conditions [7].

A sample of 90% enriched ^{235}U with a thickness of 0.0089 atoms per barn was irradiated with neutrons from the $^7\text{Li}(p,n)$ reaction. The neutron energy was determined by the time-of-flight method over 37 cm with a resolving time of 8 nsec.

The energy dependence of the coefficient α was determined from the relative yield of capture gamma rays and fission neutrons. The fast neutrons and gamma rays were recorded by three 5 x 5 cm stilbene detectors. To reduce background, the sample and the crystals were placed inside a shield containing

lead, lithium-6 and paraffin. The signals corresponding to the neutrons and the gamma rays were distinguished by the pulse shape [8]. Transmission of gamma pulses to the neutron channel did not exceed 0.01% at a pulse rate of 10^3 pulses per second.

Under these conditions the number of gamma rays N_γ and neutrons N_n recorded over a given time interval is expressed by:

$$N_\gamma = \epsilon_{\gamma c} n_e + \epsilon_{\gamma f} n_f; \quad N_n = \epsilon_n n_f$$

where n_e and n_f are the number of capture and fission events, $\epsilon_{\gamma c}$ is the efficiency of recording a capture event, and $\epsilon_{\gamma f}$ and ϵ_n are the efficiency of recording a fission event for gamma rays and neutrons respectively.

Then

$$d = \frac{n_e}{n_f} = \left(\frac{N_\gamma}{N_n} - \frac{\epsilon_{\gamma f}}{\epsilon_n} \right) / \frac{\epsilon_{\gamma c}}{\epsilon_n}$$

is determined, if $\frac{\epsilon_{\gamma c}}{\epsilon_n}$ and $\frac{\epsilon_{\gamma f}}{\epsilon_n}$ are known. For measuring $\frac{\epsilon_{\gamma f}}{\epsilon_n}$ the authors used the coincidences between fission fragments and fission gamma rays and between fragments and fission neutrons. For this purpose the uranium sample was placed throughout the experiment between two thin uranium layers (2×10^{-6} at/b) inside the gas scintillation chamber recording the fission fragments. The value of $\frac{\epsilon_{\gamma c}}{\epsilon_n}$ was obtained by normalization, using the value $\alpha = 0.375 \pm 0.032$ [6] for the neutron energy range 29-34 keV.

Pulses corresponding to fission neutrons in the energy range 0.5-8 MeV were recorded in one group of channels of an AI-4096 analyser and pulses from gamma rays in the range 0.5-3 MeV in another group. The gamma rays were detected in two ways: either by recording individual gamma rays (summation of signals from separate counters) or by recording coincidences of signals in any two out of three counters.

Measurements and results

The background was measured from the counting level in channels outside the neutron spectrum employed and was also checked by replacing the uranium sample in the chamber with a lead one. During the measurements the background was stable. In the neutron group it was 60%, 20% and 2% for neutron energies of 5, 10 and 40 keV respectively. The gamma ray background during recording of coincidences was 75, 40 and 5% for the same neutron energy values. During

recording based on the summation technique the background was 20% at 40 keV increasing with decrease in neutron energy to a level of 80% at 8 keV. Therefore, when the summation method was being used, α was not determined below neutron energies of 8 keV.

Table 1 shows the values of α obtained as well as the associated errors, which include both statistical and systematic errors with the exception of the inaccuracy in the value used at 30 keV. The data obtained using the coincidence system are in the second and third columns, whilst the summation data are in the fourth and fifth columns. The values for α in the range 5-50 keV were obtained on a continuous neutron spectrum but in the measurements at 130 keV monoenergetic neutrons were used.

The measured values of alpha were corrected for the effect of gamma ray absorption by the sample (<3%), and also for ^{238}U content in the sample (<1%). In the experiment it was assumed that the efficiency of recording gamma rays is independent of the incident neutron energy. This is in accord with the fact that the summation data agree with the coincidence data.

The results obtained here for the range 10-50 keV and 130 keV agree with the data in Refs [1, 3, 6, 10] but in the range below 10 keV the values given here are 15-25% higher than those in Refs [10, 11].

In conclusion, the authors wish to thank G.A. Otroshchenko for his assistance in the work.

Table 1

Alpha values for ^{235}U

Averaging interval keV	Coincidence method		Summation method	
5,0 - 6,0	0,38	0,11		
6,0 - 7,0	0,44	0,10		
7,0 - 8,0	0,46	0,09		
8,0 - 9,0	0,42	0,07	0,38	0,05
9,0 - 10,0	0,40	0,07	0,35	0,05
10,0 - 11,0	0,38	0,06	0,35	0,04
11,0 - 12,0	0,44	0,05	0,45	0,04
12,0 - 13,3	0,38	0,05	0,38	0,03
13,3 - 14,8	0,35	0,04	0,36	0,02
14,8 - 16,7	0,40	0,03	0,37	0,02
16,7 - 18,8	0,39	0,03	0,38	0,02
18,8 - 21,5	0,36	0,03	0,38	0,01
21,5 - 24,7	0,37	0,03	0,38	0,01
24,7 - 28,7	0,34	0,02	0,37	0,01
28,7 - 33,8	0,375	0,02	0,375	0,01
33,8 - 40,3	0,37	0,02	0,38	0,01
40,3 - 49,0	0,38	0,02	0,38	0,02
130 \pm 10	0,28	0,06	0,31	0,02

REFERENCES

- [1] HOPKINS, I.C., DIVEN, B.C., Nucl. Sci. Engng. 12 (1962) 169.
- [2] UTTLEY, C.A., AERE-M-1272 (1963).
- [3] WESTON, L.M., et al. Nucl. Sci. Engng. (1964) 20, 80.
- [4] in Physics and Chemistry of Fission (Proc. Symp. Salzburg, 1965) 1, IAEA Vienna (1965) 265.
- [5] DE SAUSSURE, G., et al. ORNL-TM (1967) 1804.
- [6] LOTTIN, A., et al. in Nuclear Data for Reactors (Proc. Conf. Paris 1966) 2, IAEA, Vienna (1967) 233.
- [7] VOROTNIKOV, P.E., et al. in Prikladnaja jadernaja spektroskopija (Applied Nuclear Spectroscopy) Atomizdat (1970).
- [8] BROVCHENKO, V.G., MOLCHANOV, Yu.D., Programme and abstracts of papers for the 20th Annual Conf. on Nuclear Spectroscopy and the Structure of the Atomic Nucleus, Part 2, Leningrad (1970) 183.
- [9] MURADYAN, G.V., et al. in Nuclear Data for Reactors (Proc. Conf. Helsinki, 1970) 1, IAEA, Vienna (1970) 357.
- [10] KUROV, M.A., RYABOV, Yu.V., et al. in Nuclear Data for Reactors (Proc. Conf. Helsinki, 1970) 1, IAEA, Vienna (1970) 345.
- [11] CZIRR, J.B., LINDSEY, J.S. in Nuclear Data for Reactors (Proc. Conf. Helsinki, 1970), 1, IAEA, Vienna (1970) 331.

ANGULAR DISTRIBUTION OF FRAGMENTS AND THE CROSS-SECTION
FOR NEUTRON-INDUCED FISSION OF ^{238}U CLOSE
TO THE THRESHOLD

P.E. Vorotnikov, S.M. Dubrovina, G.A. Otroshchenko,
V.A. Shigin

The angular distribution of fragments and the cross-section for neutron-induced fission of ^{238}U were measured in the energy range $E_n = 0.55-1.45$ MeV. The energy resolution was 20 keV and the angular resolution 12° . The measurements were performed in an electrostatic accelerator, the neutron source being a solid tritium target. The fragments were detected by glasses placed at angles of 0, 30, 60 and 90° relative to the incident neutron beam. The neutron flux was recorded with a boron counter having uniform sensitivity to the neutrons used in the measurements. The ^{238}U sample had an impurity content of $\approx 0.01\%$ ^{235}U and a deduction was made in the calculations for the effect of fission of ^{235}U . The results are shown in the tables.

Table 1

Cross-section for neutron-induced fission of ^{238}U

The relative measuring error is shown here; the absolute value of the cross-section for $E_n = 1.0$ MeV is taken from "Neutron Cross-Sections" by D.J. Hughes (BNL-325).

E_n	σ_f	$\Delta\sigma_f$	E_n	σ_f	$\Delta\sigma_f$
MeV	mb	mb	MeV	mb	mb
0,55	0,18	0,09	1,05	18,7	1,1
0,60	0,65	0,07	1,10	24,8	1,5
0,65	0,87	0,08	1,15	31,3	2,0
0,72	2,10	0,15	1,20	39,7	2,0
0,76	2,7	0,2	1,25	43,5	2
0,80	4,3	0,3	1,30	61	3
0,85	7,9	0,5	1,35	97	6
0,90	13,2	0,8	1,40	170	10
0,95	18,1	1,0	1,45	237	14
1,00	17,8	1,0			

Table 2

Angular distribution of fragments from neutron-induced fission of ^{238}U

The subscript on W denotes the mean square angle of recording of the fragments. The values given in the table are ratios of the counts of a detector set at 90° . The error for each ratio is indicated.

E_n	W_{14°	W_{34°	W_{60°	ΔW
MeV	rel. units			%
0,60	1,11	0,97	1,10	15
0,65	1,29	1,30	1,16	12
0,72	1,50	1,26	1,03	15
0,76	1,28	1,28	0,96	12
0,80	1,32	1,04	1,03	8
0,85	1,18	1,27	1,16	6
0,90	1,44	1,32	1,00	6
0,95	1,52	1,29	1,19	6
1,00	1,41	1,57	1,19	6
1,05	1,21	1,18	1,16	6
1,10	1,04	1,00	0,96	6
1,15	1,50	1,36	1,15	5
1,20	1,67	1,31	1,17	5
1,25	1,40	1,29	1,13	5
1,30	1,32	1,26	1,10	5
1,35	1,32	1,16	1,03	5
1,40	1,39	1,21	1,01	4
1,45	1,50	1,33	1,10	5

NEUTRON RESONANCES OF ^{112}Cd

Yu.G. Shchepkin, G.V. Muradyan, Yu.V. Adamchuk

Measurements have been performed to identify the S and P levels [1,2] and to establish the total cross-section, the radiative capture cross-section and the self-indication of the isotope ^{112}Cd [3, 4]. The authors have determined the orbital angular momenta for levels in the range up to 3 keV and the values of E_0 , $g\Gamma_n$ and Γ_γ up to 4 keV. (See Table 1).

A specific orbital angular momentum has been assigned to 23 of the 29 levels observed. The values of the strength functions S_0 and S_1 have been determined with allowance for the probability of identification and take the form:

$$S_0 = (0.72 \pm 0.40 / 0.23) \times 10^{-4};$$

$$S_1 = (3.9 \pm 2.9 / 2.1) \times 10^{-4}$$

The values of the radiation widths Γ_γ are found with an accuracy of $\sim 15\%$ for 12 energy levels. The mean value $\Gamma_\gamma = 80 \pm 4$ MeV is comparable with the results of calculations based on different models.

Table 1

Neutron resonance parameters of ^{112}Cd

N	E_0 eV	$g\Gamma_n^2$ meV	$\Delta(g\Gamma_n^2)$ %	Γ_γ meV	$\Delta\Gamma_\gamma$ %	χ^2/s %	K %
1	2	3	4	5	6	7	8
1.	66,91	1,16	5	52	15	100	17,4
2.	82,43	0,00485	10			50 [*])	
3.	83,27	0,0503	8			17	1,64
4.	154,4	0,00379	20			50 [*])	
5.	227,1	1,424	7	94	25	100	28
6.	284,5	0,0089	25			50 [*])	
7.	444,7	2,89	8	91	22	100	39,3
8.	455,5	0,182	10			25	3,4

* Level parity not identified.

Table 1 (continued)

I	2	3	4	5	6	7	8
9.	570,7	0,117	20			70	1,9
10.	743,3	11,16	5	77	13	100	40
11.	902,4	0,167	20			60	2,2
12.	917,9	10,22	6	79	12	100	45
13.	1064	0,318	12			15	4,1
14.	1125	22,6	6	86	14	100	30
15.	1224	0,743	15			10	9,2
16.	1355	0,925	15			0	11
17.	1443	22,6	7	88	14	100	33
18.	1662	0,54	23			88	5,5
19.	1727	10,1	5	88	15	100	51
20.	1841	0,745	18			75	7,3
21.	1983	1,35	20			0	13,2
22.	2068	37,4	9	94	16	100	25
23.	2268	0,84	35			52	7,4
24.	2384	21,5	10	95	16	100	41
25.	2498	0,8	35			60	6,6
26.	2620	32,2	9	92	16	100	31
27.	2751	40,0	7	112	16	100	27
28.	2878	1,49	25			0	12
29.	3013	8,72	27			0	49
30.	3175	8,9	30				
31.	3243	1,58	50				
32.	3315	1,04	35				
33.	3387	8,93	25				
34.	3501	1,18	30				
35.	3581	4,19	15				
36.	3791	2,11	30				
37.	3881	3,21	30				
38.	3975	4,12	23				

REFERENCES

- [1] MURADYAN, G.V., Physics Lett., 14 (1965) 123.
- [2] MURADYAN, G.V., ADAMCHUK, Yu.V., MOSKALEV, S.S., Pribory Tekh. Eksp., 6 (1966) 43.
- [3] SHCHEPKIN, Yu.G., ADAMCHUK, Yu.V., DANELYAN, L.S., MURADYAN, G.V., in Nuclear Data for Reactors (Proc. Conf. Paris 1966) 1, IAEA, Vienna (1967) 93.
- [4] MURADYAN, G.V., ADAMCHUK, Yu.V., SHCHEPKIN, Yu.G., Pribory Tekh. Eksp., 1 (1969) 28.

INVESTIGATION OF THE NEUTRON WIDTHS AND THE NEUTRON ORBITAL
ANGULAR MOMENTUM FOR LEVELS OF ^{121}Sb AND ^{123}Sb

Yu.V. Adamchuk, G.V. Muradyan, Yu.G. Shchepkin

The authors have obtained values for the neutron strength functions S_0 and S_1 . To this end measurements were performed, to determine the orbital angular momentum of the interaction of a bombarding neutron with a nucleus, using the moving sample method, and measurements were also made of the total cross-section and the neutron capture cross-section in order to determine the neutron widths.

All the measurements were performed over a 37 metre flight path [1] in the linear electron accelerator at the Atomic Energy Institute: the mean neutron yield is $\sim 2 \times 10^{12}$ n/sec and the pulse length 0.2 μsec . The resolution of the spectrometer is 11 nsec/m.

The spectrometer detector consists of two 200 x 100 mm NaI(Tl) crystals, which are shielded on the side facing the sample by a layer of boron-10 with a thickness of $\sim 4.5 \text{ g/cm}^2$.

The measurements to identify the levels in terms of the orbital angular momentum were performed using the moving sample method [2]. The velocity $V = 140 \text{ m/sec}$. The thickness of the samples used for transmission was $n_T = 0.0455 \text{ at/b}$ (^{121}Sb) and $n_T = 0.0358 \text{ at/b}$ (^{123}Sb), and of the samples in the detector $n_D = 0.0075 \text{ at/b}$ (^{121}Sb) and $n_D = 0.0067 \text{ at/b}$ (^{123}Sb) with $\sim 98.5\%$ enrichment. The measurements on each isotope lasted approximately 300 hours.

The results of the measurements were recorded in the form of a dependence of the number of counts of neutron capture events in the detector sample after transmission of the neutron beam through the moving sample.

Fig. 1 shows an example of the measurements of ^{123}Sb with curves A and B representing the movement of the sample in and against the direction of the neutron beam respectively.

When the moving sample was outside the neutron beam, measurements were made of the capture cross-section (curves C and D in Fig. 1), the latter measurements being used, firstly, for determining the level parameters, secondly for normalizing the series of measurements, which correspond to movement of the sample with and against the beam, to a single flux and, thirdly, for finding the value of the asymmetry $\Delta A_\gamma^{\text{theor}}$, assuming an S-interaction,

which is to be expected in measurements of neutron capture after passage through the moving sample. By comparing the difference in areas ΔA_Y^{exp} under the resonances on the two lower curves with the expected value of $\Delta A_Y^{\text{theor}}$ and zero, one can assign levels to S or P interactions.

The asymmetry coefficient $K = \frac{2(A_Y^{(+)\text{theor}} - A_Y^{(-)\text{theor}})}{A_Y^{(+)\text{theor}} + A_Y^{(-)\text{theor}}}$ and the ratio

$\frac{2 \cdot A_Y^{(o)\text{theor}}}{A_Y^{(+)\text{theor}} + A_Y^{(-)\text{theor}}}$ used for determining $\Delta A_Y^{\text{theor}}$ were calculated for

each level by computer. The areas under the resonances $A^{(+)\text{theor}}$, $A^{(-)\text{theor}}$ and $A^{(o)\text{theor}}$ ($A^{(o)\text{theor}}$ is the area under the resonance in the capture cross-section) were calculated in the range $\Delta E = 600 \cdot \Gamma_n \cdot \delta x$ (δx is the integration step) on the basis of measured values of Γ_n . The radiation width (Γ_γ) and the potential cross-section (σ_p) were assumed to be 100 meV and 4.3 b respectively. Tables 1 and 2 show the results of identification of levels with respect to ℓ in the form of the probability φ_s that the level is due to an S-interaction. As can be seen from the tables, ℓ was determined in the majority of cases.

Neutron width determinations and isotopic identification have been performed in Ref. [3]. In our measurements we have defined more precisely the values of $2g\Gamma_n$, for which purpose we carried out transmission measurements on the same spectrometer as our measurements to identify the levels with respect to ℓ , using the same samples and covering the additional range of 6-240 eV.

The detector used in the level identification measurements has a background approximately 3-6 times lower than that in Refs [1, 3]. Thanks to this and the accumulation of measuring statistics on capture cross-sections (curves C and D in Fig. 1) about 20 levels were identified for ^{121}Sb and ^{123}Sb .

On the basis of the level identification, the isotopic identification and the neutron width measurements, the authors calculated the neutron strength functions S_0 and S_1 .

$$S_0 = \begin{matrix} (0.20 \pm \frac{0.03}{0.02}) \cdot 10^{-4} & \text{for } Sb^{121} \\ (0.24 \pm \frac{0.00}{0.05}) \cdot 10^{-4} & \text{for } Sb^{123} \end{matrix}$$

$$S_1 = \begin{matrix} (10.1 \pm \frac{3.7}{2.8}) \cdot 10^{-4} & \text{for } Sb^{121} \\ (4.0 \pm \frac{2.5}{1.3}) \cdot 10^{-4} & \text{for } Sb^{123} \end{matrix}$$

In determining S_1 account was taken of the non-identified levels with small Γ_n by using the Porter-Thomas distribution. The error calculations allow for both statistical errors and possible errors associated with identification.

Comparison of the values obtained for S_0 and S_1 with corresponding values calculated using the optical model shows that the experimental values of S_0 are in satisfactory agreement with the calculations of Ref. [4], in which absorption is removed ~ 0.5 fermi outside the nucleus. Compared with calculations for surface absorption in Ref. [5], the S_0 values obtained here are lower by a factor of six.

The S values for ^{123}Sb agree within the error limits with calculations corresponding to the two potentials - with remote and surface absorption [4, 5]. For ^{121}Sb the experimental value of S_1 is several times in excess of the theoretical value.

The value of the parameter ν of the Porter-Thomas distribution for the system of levels with $\ell = 0$ was determined:

$\nu = 1.35 \pm 0.21$ for ^{121}Sb ($n = 93$) and $\nu = 1.07 \pm 0.29$ for ^{123}Sb ($n = 43$) (n is the number of levels, $\Delta\nu = 2/\sqrt{n}$). It was assumed that the mean values of $2g\Gamma_n^{(0)}$ are uniform for the two spin systems.

REFERENCES

- [1] MURADYAN, G.V., SHCHEPKIN, Yu.G., ADAMCHUK, Yu.V., ARUTIUNOV, M.G., Nucl. Phys., A-147, (1970) 205.
- [2] MURADYAN, G.V., Physics Lett., 14 (1965) 123.
- [3] MURADYAN, G.V., ADAMCHUK, Yu.V., SHCHEPKIN, Yu.G., Jadernaja Fizika, 8 (1968) 852.
- [4] ENGELBRECHT, C.A., FIEDELDEY, H., Ann. Phys., 42 (1967) 262.
- [5] BACK, B., PEREY, F., Phys. Rev. Lett., 8 (1962) 444.

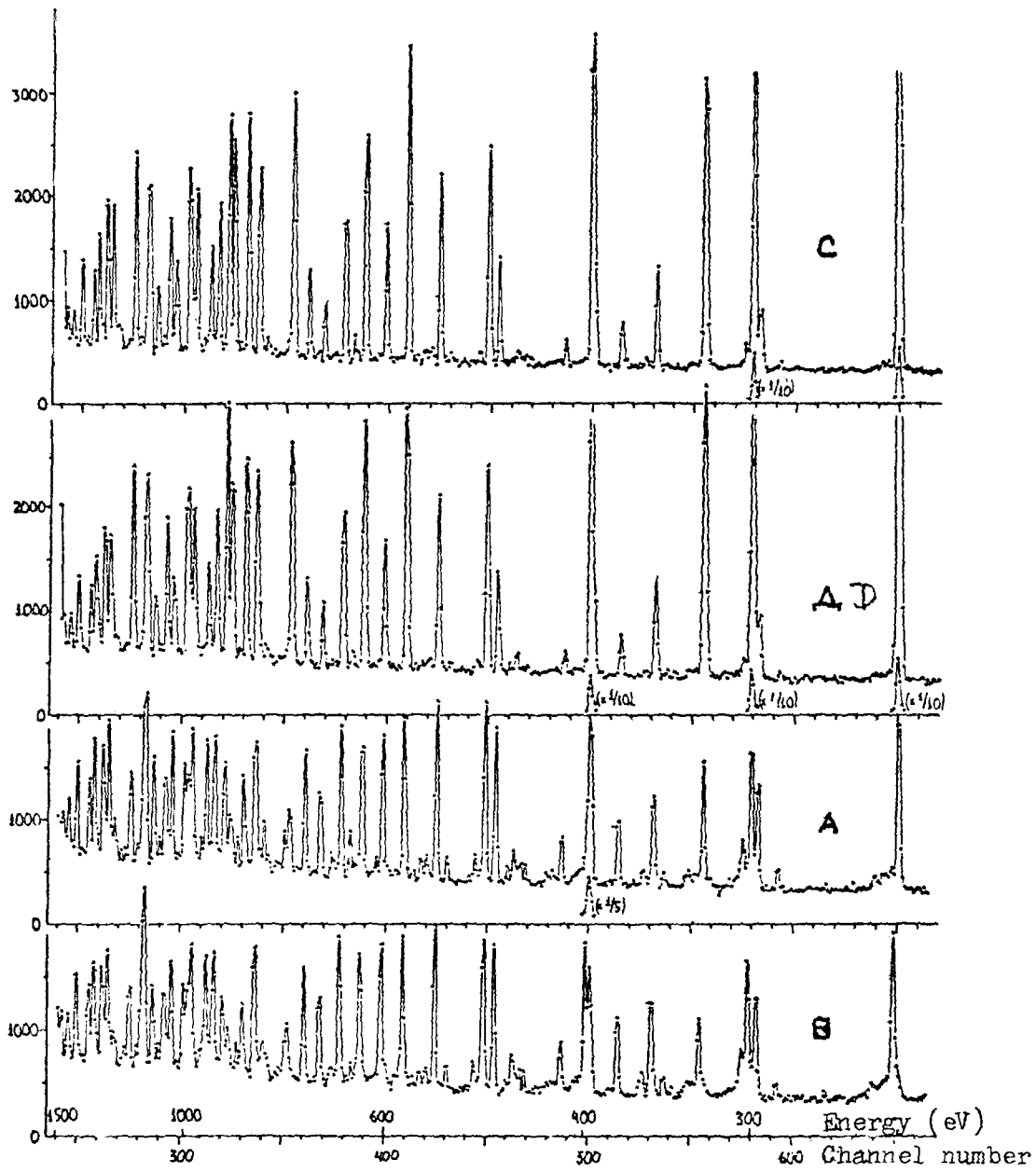


Fig. 1 Identification of ^{123}Sb levels for the orbital angular momentum of an incident neutron in the 220-1500 eV region.

Table 1

Results of measurements of ^{121}Sb

No.	E_0 eV	$2g\Gamma_n^{(e)}$ meV	$\Delta(2g\Gamma_n^{(a)})$ %	φ_s %	K %
I	2	3	4	5	6
1.	6,24	0,8	5	100	
2.	15,40	1,76	6	100	
3.	29,55	1,2	20	100	7,2
4.	37,77	0,0021	30	50 ^{*/}	-
5.	47,13	0,01	20	50 ^{*/}	-
6.	53,50	0,275	4	100	6,3
7.	55,01	0,0067	20	50 ^{*/}	-
8.	64,40	0,084	4	98	2,5
9.	73,73	0,82	6	100	11,5
10.	89,63	1,0	25	50 ^{*/}	-
11.	90,11	0,58	25	50 ^{*/}	-
12.	III,4	0,275	5	100	6,4
13.	126,6	2,4	15	100	18,6
14.	131,9	0,92	7	100	14,4
15.	144,4	1,15	15	100	16,2
16.	149,8	2,42	4	100	20,4
17.	158,8	0,0087	30	50 ^{*/}	-
18.	160,7	0,125	7	90	2,6
19.	167,0	1,43	10	100	18,4
20.	177,7	0,006	25	50 ^{*/}	-
21.	185,0	0,014	20	50 ^{*/}	-
22.	192,3	0,12	20	50 ^{*/}	-
23.	200,5	0,00035	30	50 ^{*/}	-
24.	214,2	0,086	10	55	1,4
25.	222,7	0,35	10	100	6,5
26.	228,7	0,006	30	50 ^{*/}	-
27.	230,7	0,064	10	65	1,1
28.	236,4	0,003	40	50 ^{*/}	-
29.	246,6	0,020	30	50 ^{*/}	-

Table 1 (continued)

I	2	3	4	5	6
30.	249,6	0,020	30	50 ^{*/}	-
31.	262,3	0,012	30	50 ^{*/}	-
32.	266,4	0,014	30	50 ^{*/}	-
33.	270,5	0,016	25	50 ^{*/}	-
34.	274,8	0,017	20	50 ^{*/}	-
35.	282,7 ^{*/}	0,007	50	50 ^{*/}	-
36.	287,2	0,83	10	100	13,6
37.	293,7	0,006	30	50 ^{*/}	-
38.	307,0	0,015	30	50 ^{*/}	-
39.	310,2	0,195	10	92	3,0
40.	321,2	0,032	25	50 ^{*/}	-
41.	332,1	0,141	5	63	2,0
42.	338,0 ^{*/}	0,18	40	50 ^{*/}	-
43.	339,5	0,52	10	50 ^{*/}	-
44.	348,1	0,009	20	50 ^{*/}	-
45.	355,3	0,013	25	50 ^{*/}	-
46.	363,8	0,019	25	50 ^{*/}	-
47.	393,9	1,3	10	100	18,0
48.	407,1	0,07	15	50 ^{*/}	-
49.	416,1	0,038	20	50 ^{*/}	-
50.	422,2	0,54	8	100	7,7
51.	432,6	0,0096	50	50 ^{*/}	-
52.	444,9	2,1	25	50 ^{*/}	-
53.	448,8	1,68	15	50 ^{*/}	-
54.	451,8	2,1	15	50 ^{*/}	-
55.	455,5	7,0	15	50 ^{*/}	-
56.	463,6	0,084	30	50 ^{*/}	-
57.	471,3	0,53	15	100	7,1
58.	476,6	0,028	30	50 ^{*/}	-
59.	483,3	0,068	30	50 ^{*/}	-
60.	499,2	0,38	15	80	4,9
61.	502,1	0,058	30	50 ^{*/}	-
62.	510,8	0,031	30	50 ^{*/}	-
63.	535,9	0,38	10	100	4,1
64.	544,7	4,6	8	100	32,0

Table 1 (continued)

I	2	3	4	5	6
65.	551,2	0,034	40	50% [/]	-
66.	560,4	1,0	20	100	12,7
67.	565,4	0,07	20	50% [/]	-
68.	582,1	0,04	30	50% [/]	-
69.	589,1	0,024	30	50% [/]	-
70.	601,3	0,19	15	50% [/]	-
71.	607,5	2,5	6	100	29
72.	615,2	0,52	5	35	6,2
73.	632,5	1,4	15	100	17,7
74.	647,9	0,03	30	50% [/]	-
75.	662,9	1,08	7	100	12,8
76.	672,8	1,42	10	95	17,0
77.	678,3	0,76	15	70	8,5
78.	700,0	0,03	80	50% [/]	-
79.	712,1	0,7	10	55	7,2
80.	715,8	0,09	30	50% [/]	-
81.	720,7	1,2	15	95	14
82.	731,9	0,018	40	50% [/]	-
83.	737,6	0,16	15	50% [/]	-
84.	754,0	0,01	50	50% [/]	-
85.	763,0	0,02	50	50% [/]	-
86.	774,7	2,8	10	0	27
87.	792,0	0,86	20	50% [/]	-
88.	797,7	1,9	20	50% [/]	-
89.	803,5	3,3	20	50% [/]	-
90.	805,0	2,5	30	50% [/]	-
91.	841,0	0,83	10	100	8
92.	861,5	0,52	15	95	5
93.	867,0	0,02	40	50% [/]	-
94.	892,1	0,25	20	28	2,4
95.	913,7	0,5	30	50% [/]	-
96.	919,0	4,2	20	100	32
97.	938,8	0,13	25	50% [/]	-
98.	949,8	1,4	10	100	14
99.	964,9	1,35	10	100	13

Table 1 (continued)

I	2	3	4	5	6
I00.	996,2	4,2	10	0	32
I01.	I016	1,0	15	80	9,5
I02.	I040	0,2	25	50 ^{*/}	-
I03.	I048	0,3	20	50 ^{*/}	-
I04.	I088	0,88	10	98	7,9
I05.	III3	3,6	10	100	29
I06.	II25	0,2	30	50 ^{*/}	-
I07.	II47	0,45	25	60	3,8
I08.	II80	2,8	40	} C или 100 100 или 0	24
I09.	II83	2,8	40		24
II0.	I205	1,9	15	100	16
III.	I222	0,95	20	6	8,1
II2.	I255	2,8	30	25	21
II3.	I262	0,35	20	50 ^{*/}	-
II4.	I311	2,98	10	100	23

^{*/} Level parity not identified.

^{*/} Parameters taken from Ref. [4].

Table 2

Results of measurements of ^{123}Sb

No.	E_0 eV	$2\sigma \Gamma_n^{(0)}$ meV	$\Delta(2\sigma \Gamma_n^{(0)})$ %	ψ_s %	χ %
I	2	3	4	5	6
1.	21,4	6,35	8	100	-
2.	50,5	0,39	6	100	6,6
3.	67	0,003	100	50 ^{*/}	-
4.	76,7	0,68	10	100	10,2
5.	104,9	4,15	5	100	15,4
6.	131,0	0,104	10	70	1,6
7.	176,3	0,021	20	50 ^{*/}	-
8.	186,5	0,023	20	50 ^{*/}	-
9.	191,8	1,42	10	100	16,5
10.	198,0	0,34	30	50 ^{*/}	-
11.	219,0	0,30	10	60	4,3
12.	225,8	0,021	25	50 ^{*/}	-
13.	236,4	0,02	25	50 ^{*/}	-
14.	241,0	1,3	8	98	17,7
15.	296,7	0,087	20	65	1
16.	300,0	1,39	6	100	16,8
17.	317	0,03	60	50 ^{*/}	-
18.	324,4	1,87	5	100	19,8
19.	332,1	0,062	25	50 ^{*/}	-
20.	341,5	0,034	30	50 ^{*/}	-
21.	351,5	0,332	6	88	3,93
22.	374,2	0,105	20	60	1,1
23.	392,9	0,116	20	56	1,2
24.	395,9	1,9	15	94	21,5
25.	415,4	0,070	30	50 ^{*/}	-
26.	427,6	0,015	80	50 ^{*/}	-
27.	472,6	0,194	6	70	1,98
28.	483,3	0,56	10	100	5,9
29.	492,9	0,043	25	50 ^{*/}	-
30.	522,6	0,043	30	50 ^{*/}	-

Table 2 (continued)

I	2	3	4	5	6
31.	533,5	0,556	7	100	5,62
32.	551,9	0,03	40	50*/	-
33.	572,4	1,67	20	100	17,1
34.	600,9	0,39	20	85	3,5
35.	629,4	1,3	20	100	12,6
36.	645,8	0,054	30	50*/	-
37.	660,7	0,75	10	94	6,9
38.	693,2	0,15	20	65	1,2
39.	702,6	0,034	50	50*/	-
40.	719,4	0,21	25	68	1,7
41.	749,8	7,1	10	100	34
42.	818,2	1,55	10	72	12,6
43.	842,6	3,4	10	97	26,3
44.	874,6	7,8	10	100	32,8
45.	887,9	2,9	5	100	22,2
46.	896,3	0,097	25	50*/	-
47.	911,9	0,9	20	96	6,87
48.	933,3	0,58	10	13	4,42
49.	970,7	1,12	8	100	8,71
50.	980,4	0,16	30	50*/	-
51.	990,2	2,64	10	100	19,9
52.	1031	0,44	25	88	3,08
53.	1050	1,79	10	25	13,6
54.	1036	0,36	20	50*/	-
55.	1094	0,18	30	50*/	-
56.	1113	0,72	25	50*/	-
57.	1120	2,36	10	20	17
58.	1168	2,33	6	69	18
59.	1223	0,17	35	50*/	-
60.	1239	0,14	35	50*/	-
61.	1253	1,03	15	97	8,9
62.	1276	1,3	10	99	8,65
63.	1311	0,78	15	32	4,95
64.	1333	0,52	30	43	3,23
65.	1387	0,49	20	80	2,93

* / Level parity not identified.

ELASTIC SCATTERING OF NEUTRONS BY ^{208}Pb AND THE
OPTICAL NUCLEAR MODEL

V.M. Morozov, Yu.G. Zubov, N.S. Lebedeva

Measurements were made of the differential elastic scattering cross-sections of neutrons of energy 1.8 ± 0.2 MeV by a ^{208}Pb nucleus in the scattering angle range $12-168^\circ$. The cross-section $\sigma(\vartheta)$ was obtained in a beam of neutrons emitted by the reaction $\text{D}-^{12}\text{C}$ at an angle $\alpha_{\text{rad}} = 37^\circ$ with a mean accelerated deuteron energy of 2.2 MeV. The cross-section $\sigma^\varphi(\vartheta)$ was measured in a neutron beam obtained from the first beam by passing it through a ^{208}Pb filter 124 mm thick (transparency 0.122) and differing from the first beam in that it was depleted by one or more orders of magnitude in neutrons corresponding to the resonances in the total cross-section for the interaction of neutrons with a ^{208}Pb nucleus.

The differential cross-section has a diffraction character and has no symmetry relative to 90° . Due to this some doubt is cast on the applicability of the theory concerning the existence of the two non-interfering processes of elastic scattering - potential scattering and scattering by the compound nucleus - at any rate in the range of isolated resonances of the nucleus. Attention is given to the relative displacement of the minima and maxima in the angular distributions of $\sigma(\vartheta)$, $\sigma^\varphi(\vartheta)$ and $\sigma(\vartheta) - \sigma^\varphi(\vartheta)$. The values for $\sigma(\vartheta)$, $\sigma^\varphi(\vartheta)$ and $\sigma(\vartheta) - \sigma^\varphi(\vartheta)$ are given in Table 1.

Table 1

12°	2,18	1,84	$0,34 \pm 0,06$
20°	1,84	1,53	$0,31 \pm 0,05$
30°	1,26	1,06	$0,20 \pm 0,04$
40°	0,72	0,635	$0,08 \pm 0,02$
50°	0,346	0,315	$0,031 \pm 0,01$
60°	0,147	0,144	$0,003 \pm 0,004$
70°	0,095	0,086	$0,009 \pm 0,003$
80°	0,135	0,125	$0,010 \pm 0,004$
90°	0,225	0,195	$0,030 \pm 0,006$

Table 1 (continued)

I00°	0,320	0,298	0,022 ± 0,009
I10°	0,338	0,326	0,012 ± 0,009
I20°	0,319	0,309	0,010 ± 0,009
I30°	0,236	0,244	0,008 ± 0,007
I40°	0,184	0,167	0,017 ± 0,005
I50°	0,186	0,146	0,040 ± 0,005
I60°	0,247	0,180	0,067 ± 0,006
I68°	0,314	0,223	0,091 ± 0,008

The statistical accuracy of measuring the cross-sections is ~ 2%. The absolute values of the cross-sections $\sigma(\vartheta)$ and $\sigma^\Phi(\vartheta)$ are determined relative to each other with an accuracy of ~ 4%. The accuracy of determining the absolute values of cross-sections is 7%.

THE SENSITIVITY OF THE THERMAL UTILIZATION FACTOR TO VARIATIONS IN MACROSCOPIC CROSS-SECTIONS

N.I. Laletin

Estimates are made of the effect (influence factor) of different macroscopic cross-sections on the thermal utilization factor. This is determined as $K(\vartheta; \Sigma_i) = \frac{\delta \vartheta}{\vartheta} / \frac{\delta \Sigma_i}{\Sigma_i}$. A one-velocity approximation is used. Simple formulae are obtained which provide a means of performing quantitative evaluations for a wide range of nuclei. The basic formulae are:

$$K(\vartheta; \Sigma_{af}) \cong -\frac{1-\theta}{\alpha}, \quad (1)$$

$$K(\vartheta; \Sigma_{am}) \cong (1-\theta), \quad (2)$$

$$K(\vartheta; \Sigma_{s,f}) \cong 0,4(1-\theta) \frac{Q-1}{\alpha} \cdot \frac{\Sigma_{s,f}}{\Sigma_f}, \quad (3)$$

$$K(\vartheta; \Sigma_{sm}) \cong 0,5 \frac{\bar{\Phi}_m - \Phi_{b0}}{\bar{\Phi}_m} (1-\theta), \quad (4)$$

$$K(\vartheta; \Sigma_{sm}^{(0)}) \cong (1-\theta) \bar{\mu} \frac{\bar{\Phi}_m - \Phi_{b0}}{\bar{\Phi}_m} \approx 0,5, \quad (5)$$

$$K(\vartheta; \Sigma_{sm}^{(n)}) \cong 0,05 \bar{\mu} (1-\theta) \quad (6)$$

The following notation is employed:

- ϑ is the thermal utilization factor;
- $d = \frac{\bar{\Phi}_m}{\bar{\Phi}_f}$ is the ratio of the mean flux in the moderator $\bar{\Phi}_m$ to the mean flux in the fuel $\bar{\Phi}_f$ (disadvantage factor);
- Σ_{af} is the fuel absorption cross-section;
- Σ_{am} is the moderator absorption cross-section;
- $Q = \frac{\Phi_{b0}}{\Phi_f}$ is the shielding constant of the fuel element;
- Φ_{b0} is the neutron flux at the fuel element boundary;
- Σ_{sf} Σ_f are the scattering cross-section and the total cross-section for neutron interaction in the fuel; Σ_{sm} and Σ_m are similar values for the moderator; $\Sigma_{sm}^{(n)}$ is the n^{th} angular momentum of the scattering cross-section in the fuel and $\bar{\mu}$ is the mean cosine of the scattering angle in the fuel.

THE EFFECT OF VARIATION IN MICROSCOPIC CROSS-SECTIONS
FOR NEUTRON INTERACTION ON THE INTEGRAL
CHARACTERISTICS OF A THERMAL NEUTRON SPECTRUM

G.Ya. Trukhanov

To formulate accuracy requirements for nuclear data in reactor construction, it is necessary to have an idea of the sensitivity of the integral characteristics of neutron distribution (used directly in the design of nuclear reactors) to variations in the microscopic cross-sections for neutron interaction with a substance. The solution of this problem as a whole for reactor construction must be preceded by work to assess the sensitivity of the integral parameters to errors in nuclear data for various types of reactor systems.

In this paper the author studies the effect of variations in the microscopic cross-sections for neutron interaction with a substance on the integral characteristics of a thermal neutron spectrum in the case of a plane uranium-water-graphite cell (thickness of the graphite 15 cm, of the water 0.5 cm and of the uranium slug 1.5 cm), which is characterized by the temperature non-uniformities ($T_c = 893^\circ\text{K}$; $T_{\text{H}_2\text{O}} = 353^\circ\text{K}$). The nuclear constants were taken from Hughes' Atlas [1]. A quantitative evaluation of the sensitivity of the integral parameters to variations in microscopic cross-section was performed by applying an influence factor, introduced via the relation:

$$\frac{\delta X}{X} = K(X, \beta) \frac{\delta \beta}{\beta}$$

where $\delta\beta$ and $\delta\chi$ are variations of the constant β and the corresponding variations of χ . Calculation of the space-energy distribution of thermal neutrons in the cell and calculation on this basis of the integral values for given microscopic interaction cross-sections was performed on the basis of the "DEMETRA" thermalization programme [2, 3].

The results of the analysis are given in Table 1.

Table 1

The effect of variations in nuclear data on the thermal utilization factor ρ in a uranium-water-graphite cell

Variable parameters	$\frac{\delta\beta}{\beta}, \%$	$K(\theta, \beta)$		Variable parameters	$\frac{\delta\beta}{\beta}, \%$	$K(\theta, \beta)$	
		P_I - approximation	Quasi-diffusion solution			P_I - approximation	Quasi-diffusion solution
1	2	3	4	5	6	7	8
ρ_c	-15,4	+0,022	+0,023	$\sigma_{u^{238}}$	-4,4	-0,009	-0,009
	-9,4	+0,022	+0,020		-1,46	-0,009	-0,009
	+9,6	-0,022	-0,021		+1,46	+0,009	+0,009
	+15,5	-0,022	-0,023		+4,4	+0,009	+0,009
ρ_H	-0,61	+0,035	+0,039	σ_s^e	-8,4	+0,013	+0,012
	+0,61	-0,035	-0,039		+8,4	-0,013	-0,012
	+1,5	-0,035	-0,039				
$\rho_{u^{235}}$	-1,00	-0,016	-0,017	σ_s^H	-19	+0,009	+0,0095
	-0,32	-0,016	-0,018		+19	-0,009	-0,0095
	+0,32	+0,016	+0,018				
	+1,00	+0,016	+0,017				

Note

- $\chi = \sigma_a(v_T) \cdot v_T [\text{barn} \cdot \text{eV}^{1/2}]$, where $\sigma_a(v_T)$ is the microscopic absorption cross-section in barns, v_T is the thermal neutron velocity in $\text{eV}^{1/2}$.
- σ_s is the microscopic scattering cross-section.

From the results in Table 1 the following conclusions can be drawn:

1. The sensitivity of β to variations in the microscopic cross-sections for neutron interaction with a substance is very low for systems of the type considered;
2. The influence factors are constant over a wide range of nuclear data values, which extends well beyond the limits of experimental error;
3. The P_I -approximation gives qualitatively and quantitatively correct values of the influence factors.

REFERENCES

- [1] HUGHES, D., SCHWARTZ, R., Atlas nejtronnyh sečenij (Neutron Cross-section Atlas), Moscow, Atomizdat (1959).
- [2] TRUKHANOV, G.Ya., Rešenje zadač termalizacii metodom kvazidiffuzii (Solution of thermalization problems by the quasi-diffusion method), Institute of Atomic Energy preprint, IAE-1875 (1969).
- [3] TRUKHANOV, G.Ya., Kompleks programm rasčeta zadač termalizacii nejtronov v odnomernoj jačejke geterogennogo reaktora metodom kvazidiffuzii (Set of programmes for calculating neutron thermalization problems in a unidimensional cell of a heterogeneous reactor by the quasi-diffusion method - "DEMETRA"), Institute of Atomic Energy preprint, IAE-2010 (1970).

NEUTRON FLUX RELAXATION LENGTHS AND RETHERMALIZATION LENGTHS IN GRAPHITE AND WATER

G.Ya. Trukhanov, Yu.A. Safin

The authors present the results of an analysis of experiments on neutron thermalization in a graphite-water system having a temperature jump over a wide range of graphite temperatures from 133 to 823^oK, which were performed in the I.V. Kurchatov Atomic Energy Institute over a number of years [1, 2]. The method of measurement and the processing of experimental data are described in detail in Ref. [1]. The method of deriving the first relaxation length and the rethermalization length from the experimental data is explained in Ref. [3].

Table 1 shows the relaxation lengths of neutrons in water. The values obtained for the first relaxation length L_1 are considerably less than the

maximum possible value for water $\frac{1}{x^*} = 0.74$ cm. On the one hand, this can mean that in water there is only a fundamental relaxation length, and the values of L_1 obtained are the result of an attempt to describe a continuous spectrum of eigenvalues with one discrete eigenvalue. On the other hand, the fact that they all come within a specific range (0.27-0.37 cm) may indicate that a quasi-discrete relaxation length exists in the region of the continuous spectrum for water in the same way as quasi-discrete damping constants can exist in the non-stationary thermalization problem [4].

Table 2 shows neutron rethermalization lengths in graphite. It can be seen that the rethermalization length in graphite strongly depends on graphite temperature which is a reflection of the effect of chemical bonds in the graphite. The neutron rethermalization lengths in water are given in Table 3. No specific dependence on the temperature of the neighbouring zone is to be observed. In addition, the rethermalization properties of water were calculated. The differential scattering cross-sections were calculated in accordance with the Nelkin model [5]. The results of the calculation are given in Table 4. The neutron rethermalization lengths in water, obtained on the basis of the Nelkin model, do in fact depend, if only very slightly, on the temperature of the neighbouring zone.

REFERENCES

- [1] MAIOROV, L.V., MOSTOVOY, V.I., SAFIN, Yu.A., TRUKHANOV, G.Ya., in Pulsed Neutron Research (Proc. Symp. Karlsruhe, 1965) 1, IAEA, Vienna (1965) 657.
- [2] ABDULLAEV, Kh.Sh., BRYZGALOV, V.I., DIKAREV, V.S., LIMAN, G.F., MAIOROV, L.V., MOSTOVOY, V.I., TARABANKO, V.A., in Neutron Thermalization and Reactor Spectra (Proc. Symp. Ann Arbor, 1967) 2, IAEA, Vienna (1968) 233.
- [3] ABDULLAEV, Kh.Sh., NIKITIN, V.D., TRUKHANOV, G.Ya., Dliny relaksacii v vode (Relaxation lengths in water) Institute of Atomic Energy preprint, IAE-1612 (1968).
- [4] KAZARNOVSKY, M.V., et al., in Neutron Thermalization and Reactor Spectra (Proc. Symp. Ann Arbor, 1967) 2, IAEA, Vienna (1968) 331.
- [5] NELKIN, M., Phys. Rev. 119 (1960) 741.

Table 1

Relaxation lengths in water

No. of exp.	I	2	3	4	5	6
$T_c, ^\circ K$	133	133	443	594	725	823
$T_{H_2O}, ^\circ K$	297	343	298	302	305	305
L_λ	$0,29 \pm 0,03$	$0,30 \pm 0,03$	$0,37 \pm 0,04$	$0,43 \pm 0,04$	$0,36 \pm 0,04$	$0,40 \pm 0,04$
L_I	$0,27 \pm 0,03$	$0,27 \pm 0,03$	$0,33 \pm 0,03$	$0,37 \pm 0,04$	$0,32 \pm 0,04$	$0,35 \pm 0,03$

Table 2

Rethermalization lengths in graphite

	I	2	3	4	5	6
$T_C, ^\circ K$	133	133	443	594	725	823
$T_{H_2O}, ^\circ K$	297	343	298	302	305	305
$T_I, ^\circ K$	155	155	454	596	726	830
L_λ, cm	18 ± 3	$15,6 \pm 3,2$	$7,4 \pm 0,7$	$6,3 \pm 0,6$	$5,1 \pm 0,5$	$4,9 \pm 0,5$
L_{rt}, cm	10 ± 1	$9,2 \pm 1,1$	$5,5 \pm 0,6$	$4,9 \pm 0,5$	$4,1 \pm 0,4$	$4,0 \pm 0,4$

Table 3

Rethermalization lengths in water

	1	2	3	4	5	6
$T_C, ^\circ K$	133	133	443	594	725	823
$T_{H_2O}, ^\circ K$	297	343	298	302	305	305
$T_2, ^\circ K$	307	356	303	310	310	315
L_{τ}, cm	$0,30 \pm 0,03$	$0,47 \pm 0,05$	$0,52 \pm 0,05$	$0,44 \pm 0,04$	$0,45 \pm 0,04$	$0,48 \pm 0,05$
L_{rt}, cm	$0,26 \pm 0,03$	$0,41 \pm 0,04$	$0,44 \pm 0,04$	$0,38 \pm 0,04$	$0,39 \pm 0,04$	$0,41 \pm 0,04$

Table 4

Rethermalization characteristics of water
(Nelkin model)

$T_1, ^\circ K$	$T_2, ^\circ K$	$T_{H_2O}, ^\circ K$	L_{D1}, cm	D_1, cm	$\sum_{S1}, \text{cm}^{-1}$	$\sum_{R}^{1 \rightarrow 2}, \text{cm}^{-1}$	L_{rt}, cm
155	307	297	3,00	0,123	3,73	0,735	0,339
155	356	343	3,12	0,119	3,74	0,821	0,374
380	310	304	2,99	0,187	2,82	0,689	0,514
453	305	300	2,83	0,189	2,72	0,765	0,491
596	310	300	2,85	0,201	2,54	0,748	0,514
725	310	300	2,85	0,211	2,41	0,724	0,534
833	310	300	2,85	0,217	2,35	0,710	0,547

JOINT INSTITUTE OF NUCLEAR RESEARCH

EXTRACTION OF ULTRA-COLD NEUTRONS FROM A REACTOR

V.V. Golikov, V.I. Lushchikov, F.L. Shapiro

The authors calculate the yield of ultra-cold neutrons from different sources (converters) of temperature T_K irradiated with an isotropic thermal neutron flux having a Maxwellian spectrum of temperature T_n . The results of the calculations of the dependence of the ultra-cold neutron flux on the temperature of a number of converters, T_K , for a fixed neutron spectrum temperature ($T_n = 300^\circ\text{K}$) are given in Fig. 1.

For polyethylene, beryllium and zirconium hydride (curves 1, 2 and 3 respectively), the ultra-cold neutron yield increases noticeably with cooling of the converter. The ultra-cold neutron yield from magnesium (curve 4), however, depends only slightly on the converter temperature. The results of the calculations are comparable with those of experiments performed on the ultra-cold neutron channel of the IBR-30 pulsed reactor. Cooling of the polyethylene converter from room temperature ($T = 300^\circ\text{K}$) to $T_K = 130^\circ\text{K}$ and $T_K = 90^\circ\text{K}$ caused the ultra-cold neutron flux to increase by factors of 2.2 ± 0.2 and 4 ± 0.2 respectively, which is slightly less than the theoretical values of 3 and 5.5.

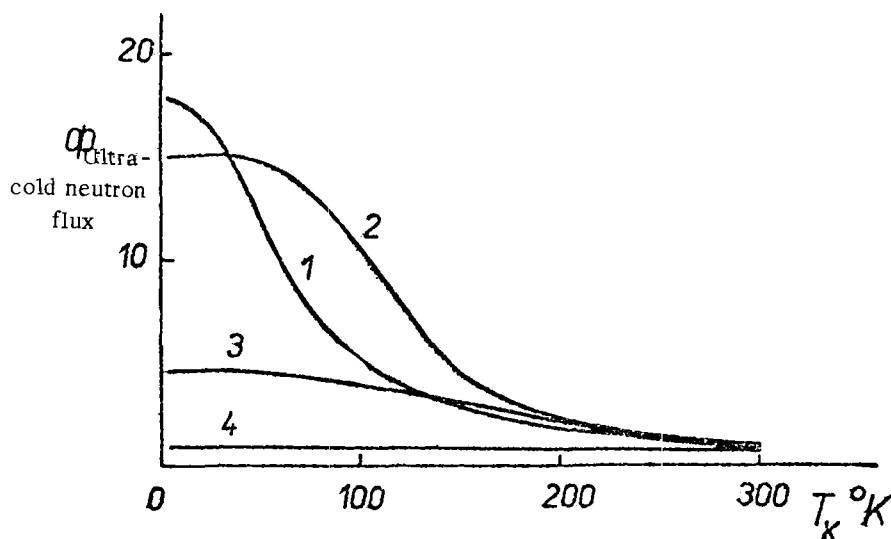


Fig. 1.

EXPERIMENTS WITH ULTRA-COLD NEUTRONS

L.V. Groshev, V.N. Dvoretzky, A.M. Demidov, Yu.N. Panin
V.I. Lushchikov, Yu.N. Pokotilovsky, A.V. Strelkov, F.L. Shapiro

(JINR Preprint, RZ-5392, 1970; Physics Lett. 34B, 4 (1971) 293)

It is shown how ultra-cold neutrons can be extracted from a stationary reactor through curved reflecting neutron tubes.

The ultra-cold neutron flux at the end of the tube was several neutrons per second, which corresponds to the theoretically predicted value. The background from residual neutrons at the point of installation of the ultra-cold neutron detector was 10% of the total count.

In the neutron tube, made of electropolished copper tubes 10 cm in diameter, the diffusion length was measured as 4.7 ± 0.1 M, which corresponds to the probability of diffuse and mirror reflection of neutrons on the wall of the neutron tube being in the ratio 1:9. The method of raising the neutron tube in the field of gravity was used to measure the ultra-cold neutron spectra at the tube outlet. By measuring the ultra-cold neutron counting rate as a function of the helium pressure in the neutron tube it was possible to estimate the mean source-to-detector time (~ 5 sec for a length of 6 m).

Direct measurements were made of the confinement time in closed volumes of the order of 30 litres with walls made of beryllium, pyrographite, copper, stainless steel etc. According to preliminary data the confinement time in these volumes does not exceed 30 sec in the range of wall temperature variation from -190°C to $+400^{\circ}\text{C}$.

NEUTRON RESONANCES OF THE ISOTOPES SAMARIUM-147 AND 149

E.N. Karzhavina, A.B. Popov

The LNF neutron spectrometer of the Joint Institute of Nuclear Research, which has a resolution of 6 nsec/m, was used to measure the transmission and yield of gamma rays from neutron capture on samples of samarium with different isotopic composition. Isotopic identification was performed and the resonance parameters of ^{147}Sm and ^{149}Sm were determined in the ranges up to 400 eV and 250 eV respectively.

Values for D - the mean distances between resonances for ^{147}Sm and ^{149}Sm - were obtained as (7.2 ± 0.9) eV; (2.3 ± 0.3) eV and for S_0 - the strength functions - as $(3.7 \pm 0.8) \times 10^{-4}$ and $(5.1 \pm 0.9) \times 10^{-4}$.

Table 1

Neutron resonance parameters of ^{147}Sm

E_0 , eV	Γ , meV	$2g\sqrt{\Gamma}$, meV	Γ_r , meV	$2g\sqrt{\Gamma}$
18,3 \pm 0,1		62 \pm 7		14,5 \pm 1,6
27,1		4,2 \pm 0,2		0,81 \pm 0,08
29,7	75 \pm 16	14 \pm 2	61 \pm 16	2,6 \pm 0,4
32,1	113 \pm 25	35 \pm 7	78 \pm 26	6,2 \pm 1,2
39,7		80 \pm 11		12,7 \pm 1,7
40,6 \pm 0,1		(2,4)		(0,38)
49,3 \pm 0,2	66 \pm 17	17 \pm 3	49 \pm 17	2,4 \pm 0,4
57,9 \pm	85 \pm 7	44 \pm 5	41 \pm 9	5,8 \pm 0,7
64,9		14 \pm 2		1,7 \pm 0,3
76,0	62 \pm 9	23 \pm 4	39 \pm 10	2,6 \pm 0,5
79,8		2,8 \pm 0,3		0,31 \pm 0,03
83,4 \pm 0,2	95 \pm 7	60 \pm 6	35 \pm 9	6,6 \pm 0,7
94,9 \pm 0,3		17 \pm 4		1,7 \pm 0,4
99,5		290 \pm 44		29 \pm 5
102,6		145 \pm 20		14 \pm 2
106,8		31 \pm 6		3,0 \pm 0,6
108,4		(0,8)		(0,08)
123,4 \pm 0,3	174 \pm 9	136 \pm 10		12,2 \pm 0,9
140,0 \pm 0,4		77 \pm 8		6,5 \pm 0,7
143,3		2,0 \pm 0,2		0,17 \pm 0,02
151,3 \pm 0,4		134 \pm 14		11 \pm 1
160,8 \pm 0,5		90 \pm 10		7,1 \pm 0,8
163,6		88 \pm 10		6,9 \pm 0,8
171,7		12 \pm 2		0,92 \pm 0,15
179,7		3,0 \pm 0,3		0,22 \pm 0,02
183,7		420 \pm 40		31 \pm 3
190,8		9,4 \pm 1,4		0,68 \pm 0,10
193,5		2,6 \pm 0,6		0,19 \pm 0,04
198,0 \pm 0,5		8,4 \pm 0,9		0,60 \pm 0,06
205,8 \pm 0,6		184 \pm 22		12,8 \pm 1,5
221,6		110 \pm 16		7,4 \pm 1,1
225,3		140 \pm 16		9,3 \pm 1,1
228,6		2,5 \pm 0,4		0,17 \pm 0,03
240,6 \pm 0,6		13 \pm 2		0,84 \pm 0,13
247,7 \pm 0,7		120 \pm 14		7,6 \pm 0,9
256,5 \pm 0,7		135 \pm 16		8,4 \pm 1,0
263,5 \pm 0,8		(55)		(3,4)
265,8		(112)		(6,9)
271,0		(36)		(2,2)
274,4		9 \pm 3		0,54 \pm 0,18
283,3 \pm 0,8		28 \pm 5		1,7 \pm 0,3
289,4 \pm 0,9		(25)		(1,5)
290,5		(25)		(1,5)
308,0		5,0 \pm 1,2		0,28 \pm 0,07
312,0 \pm 0,9		12 \pm 4		0,7 \pm 0,2
321 \pm 1		7 \pm 2		0,4 \pm 0,1

Table 1 (continued)

E_0 , eV	Γ , meV	$2g\Gamma_n$, meV	Γ_n , meV	$2g\Gamma_n^0$
330 } 332 }		160 \pm 25		8,8 \pm 1,4
340		76 \pm 12		4,1 \pm 0,6
350		57 \pm 8		3,0 \pm 0,4
359 \pm 1 }		270 \pm 30		14,2 \pm 1,6
379 \pm 1,2		350 \pm 80		18 \pm 4
382 \pm 1,2		(12)		(0,61)
391 \pm 1,3		102 \pm 22		5,3 \pm 1,1
398 } 399 \pm 1,3 }		(110)		(5,5)
406 \pm 1,4		17 \pm 6		0,24 \pm 0,30
412 \pm 1,4		44 \pm 8		2,2 \pm 0,4
419 \pm 1,5		94 \pm 30		4,6 \pm 1,5
423 \pm 1,5		29 \pm 9		1,4 \pm 0,4

Table 2

Neutron resonance parameters of ^{149}Sm

E_0 , eV	$2g\Gamma_n$, meV	$2g\Gamma_n^0$, meV
15,8 \pm 0,1	0,32 \pm 0,04	0,08 \pm 0,01
17,1	2,8 \pm 0,4	0,68 \pm 0,10
23,2	1,2 \pm 0,2	0,25 \pm 0,04
24,6	(0,36)	(0,07)
25,2	24 \pm 7	4,8 \pm 1,4
26,1	5,0 \pm 0,7	0,98 \pm 0,14
27,9	0,30 \pm 0,06	0,06 \pm 0,01
29,9	4,7 \pm 1,6	0,86 \pm 0,29
30,7	17 \pm 4	3,1 \pm 0,7
33,9	10 \pm 2	1,7 \pm 0,3
40,1	28, \pm 5	4,4 \pm 0,8
41,3	38 \pm 7	5,9 \pm 1,1
44,3	90 \pm 27	13,5 \pm 4,1
45,1 \pm 0,1	23 \pm 6	3,4 \pm 0,9
49,5 \pm 0,2	16 \pm 3	2,3 \pm 0,4
50,5	2,2 \pm 0,4	0,31 \pm 0,06
51,6	51 \pm 20	7,1 \pm 2,8
57,4	30 \pm 9	4,0 \pm 1,2
59,7	90 \pm 20	11,6 \pm 3
60,9	2,3 \pm 0,6	0,30 \pm 0,08
62,1	61 \pm 11	7,7 \pm 1,4
64,7	98 \pm 33	12,2 \pm 4,1
68,3	27 \pm 7	3,3 \pm 0,8
70,8	96 \pm 40	11,4 \pm 4,7
72,2		
73,1	(130)	(15)
74,6	29 \pm 6	3,4 \pm 0,7

Table 2 (continued)

E_0 , eV	$2q\Gamma_n$ meV	$2q\Gamma_n^0$ meV
75,3	30 ± 6	$3,5 \pm 0,7$
$76,9 \pm 0,2$	$4,5 \pm 0,8$	$0,51 \pm 0,09$
$83,8 \pm 0,2$	20 ± 5	$2,2 \pm 0,5$
$87,7 \pm 0,3$	22 ± 4	$2,3 \pm 0,4$
90,6	64 ± 36	$6,7 \pm 3,8$
92,1	57 ± 17	$5,9 \pm 1,8$
95,6 } 96,3 }	(130)	(13)
98,1	(22)	(2,2)
99,5	(12)	(1,2)
101,6	$2,8 \pm 0,5$	$0,28 \pm 0,05$
104,7	20 ± 4	$2,0 \pm 0,4$
107,0	12 ± 2	$1,2 \pm 0,2$
109,0	16 ± 3	$1,5 \pm 0,3$
111,2	13 ± 2	$1,2 \pm 0,2$
115,1	10 ± 2	$0,93 \pm 0,20$
117,0	$3,2 \pm 1,2$	$0,29 \pm 0,11$
119,4	19 ± 4	$1,7 \pm 0,4$
121,7	$1,7 \pm 0,8$	$0,15 \pm 0,07$
125,2	33 ± 8	$2,9 \pm 0,7$
127,1	$2,6 \pm 0,4$	$0,23 \pm 0,04$
$130,3 \pm 0,3$	$4,7 \pm 0,6$	$0,42 \pm 0,05$
$134,1 \pm 0,4$	180 ± 60	15 ± 5
138,6	$0,8 \pm 0,2$	$0,07 \pm 0,02$
141,0	$1,7 \pm 0,3$	$0,14 \pm 0,03$
144,2	31 ± 6	$2,6 \pm 0,5$
145,7 } 146,9 }	(160)	(13)
149,5	$7,6 \pm 1,4$	$0,62 \pm 0,12$
154,7	54 ± 16	$4,3 \pm 1,3$
157,5	19 ± 4	$1,5 \pm 0,3$
$158,7 \pm 0,4$	$4,0 \pm 0,5$	$3,2 \pm 0,4$
$168,3 \pm 0,5$	20 ± 4	$1,5 \pm 0,3$
173,5	(3,6)	(0,27)
174,7	(3,6)	(0,27)
177,8	(70)	(5,3)
179,9	(70)	(5,3)
185,4	52 ± 48	$3,8 \pm 3,5$

Table 2 (continued)

$E_0, \text{ eV}$	$2g\Gamma_n \text{ meV}$	$2g\Gamma_n^0 \text{ meV}$
188,0	44 ± 26	$3,2 \pm 1,9$
192,9	12 ± 3	$0,87 \pm 0,22$
195,0	$2,2 \pm 0,4$	$0,16 \pm 0,03$
$197,4 \pm 0,5$	20 ± 6	$1,4 \pm 0,4$
$201,1 \pm 0,6$	(8,0)	(0,56)
203,7	44 ± 26	$3,1 \pm 1,8$
210,9	10 ± 2	$0,69 \pm 0,14$
214,7	17 ± 5	$1,2 \pm 0,3$
218,2	9 ± 2	$0,61 \pm 0,14$
225,6	31 ± 10	$2,1 \pm 0,7$
228,2	25 ± 8	$1,6 \pm 0,5$
230,1	52 ± 30	$3,4 \pm 2,0$
234,0	8 ± 3	$0,5 \pm 0,2$
$238,4 \pm 0,6$	(8,0)	(0,52)
$240,1 \pm 0,7$	14 ± 3	$0,9 \pm 0,2$
244,3	30 ± 11	$1,9 \pm 0,7$
248,7	18 ± 5	$1,1 \pm 0,3$

TOTAL ALPHA WIDTHS OF NEUTRON RESONANCES

Yu.P. Popov, M. Pshitula, R.F. Rumi, V.G. Semenov,
M. Stempinsky, M. Florek, V.I. Furman

Results are given of an investigation of the (n, α) reaction for target nuclei of ^{64}Zn , ^{67}Zn and ^{177}Hf . Alpha decay was observed from resonance states arising after capture of a neutron of energy 2637 eV by a ^{64}Zn nucleus ($\Gamma_\alpha \sim 4 \times 10^{-4}$ eV), of energy 1548 eV by a ^{67}Zn nucleus ($\Gamma_\alpha \sim 12 \times 10^{-4}$ eV) and of energies 1.09, 2.38, 5.89, 6.57 and 8.87 eV by a ^{177}Hf nucleus (Γ_α in the range from $1 \cdot 10^{-9}$ to 5×10^{-9} eV). These data and the previously measured values of the alpha widths $\langle \Gamma_\alpha \rangle$ (or the upper estimates) for ten isotopes in the mass number range $95 \leq A \leq 189$ are comparable with the results of calculations based on an optical nuclear model. The fluctuations of the total alpha widths are analysed and it is shown how the resonance spins can be determined from the total alpha widths. The authors supply the distribution of the Γ_α - widths and the results of spin identification of resonances for a ^{147}Sm nucleus based on recent measurements with a neutron energy resolution of 40 nsec/m. $\ell = 3$ is assigned to the following resonances: 3.4, 27.1, 29.7, 40.6, 83.4, 102.6, 123.4, 160.8, 183.7, 190.8 and 198.0 eV.

DISTRIBUTION OF PARTIAL ALPHA WIDTHS OF NEUTRON RESONANCES

I. Vilgelm, Yu.P. Popov, M. Pshitula, R.F. Rumi
M. Stempinsky, M. Frontaseva

The paper presents the results of an analysis of distributions of experimentally determined partial alpha widths for neutron resonances of ^{147}Sm and ^{143}Nd . Assuming that partial alpha widths are subject to a chi-square distribution, the authors obtained from experimental data the number of degrees of freedom for the distribution of alpha widths in the transition to the ground state of a daughter nucleus: $\nu_{\text{ex}} = 0.62 \pm 0.15$ for eight resonances of ^{147}Sm and $\nu_{\text{ex}} = 1.3 \pm 0.4$ for five resonances of ^{143}Nd . For the distribution of partial alpha widths in the transition to the first excited state in the case of ^{147}Sm resonances a value of $\nu_{\text{ex}} = 4.9 \pm 2.1$ was obtained, which indicates that the fluctuations of the reduced alpha widths are independent of the various orbital angular momenta l , participating in the transition. The theoretical value of ν in the first two cases above is unity and in the other case 1.9.

OPTICAL MODEL ANALYSIS OF THE (n, α) REACTION

V.I. Furman, Yu.P. Popov

The (n, α) reaction, studied in terms of resonance neutrons, is the only source of information on mean alpha particle widths for nuclei with mass numbers of $A > 50$ [1]. Since the mean alpha widths are considerably smaller than the mean neutron and radiation widths (1) we can write with good accuracy

$$(T_{\alpha f e}^J)_{\text{om}} = 1 - |U_{\alpha f e}^J|^2 = 2\pi \frac{\langle \Gamma_{\alpha f e}^J \rangle}{D^J} \quad (1)$$

where $(T_{\alpha f e}^J)_{\text{om}}$ is the transmission coefficient of the optical model (OM), l is the orbital angular momentum of the alpha particles, $U_{\alpha f e}^J$ is the scattering matrix, $\langle \Gamma_{\alpha f e}^J \rangle$ is the mean experimental alpha width for the levels of a compound nucleus with spin J , D^J is the distance between these levels, and f numbers the excitation levels of the daughter nucleus. In the case of s-neutrons there are two compound nucleus spins, and the total width is obtained from (1) as:

$$\langle \Gamma_{\alpha} \rangle = \frac{1}{N} \sum_{\lambda=0}^{\infty} \sum_{\ell} \Gamma_{\lambda \ell} = \langle \Gamma_{\alpha} \rangle_{\text{OM}} = \frac{\pi}{2\pi} \sum_{\ell} \left\{ \sum_{\ell} T_{\alpha \ell}^{J+} + \sum_{\ell} T_{\alpha \ell}^{J-} \right\} \quad (2)$$

Here N is the total number of levels and D_H is the mean distance between them. In view of the strong energy dependence of the alpha widths it is convenient to introduce the strength function:

$$S_{\alpha\ell}^J = \frac{\sum_{\ell} \langle \Gamma_{\alpha\ell}^J \rangle}{2D^0 \sum_{\ell} P_{\alpha\ell}} = (S_{\alpha\ell}^J)_{OM} = \frac{\sum_{\ell} T_{\alpha\ell}^J}{4\pi \sum_{\ell} P_{\alpha\ell}} \quad (3)$$

where $P_{\alpha\ell}$ is the penetration factor with allowance for the nuclear potential. For calculating $\langle \Gamma_{\alpha\ell} \rangle_{OM}$ and $(S_{\alpha\ell}^J)_{OM}$ it is necessary to use the optical potential (OP) with smooth dependence of the parameters on A , which enables the results for different nuclei to be compared. We use the theoretical alpha-particle OP [2], since no "unique" phenomenological potential exists. In this case the OP for alpha particles is obtained by averaging the single-nucleon phenomenological OP over the nucleon distribution density in an alpha particle. The real part of the potential obtained in this way is approximated by the Woods-Saxon potential with variable diffusivity $a(R)$. For $A > 40$

$$\alpha(R) = 0.69 + 0.24 \exp\{-[(R - R_{ov})/4.75]^2\}; \quad R_{ov} = r_{ov} A^{1/3} \quad (4)$$

The corresponding depth is obtained automatically as $V_{\alpha} = K_v(A) \sum_{i=1}^4 V_{oi}$; here $K_v(A)$ is the renormalization coefficient from Ref. [2], and V_{oi} are the depths of the single-nucleon OP. Taking the parameters of the single-nucleon potentials from Ref. [3], we arrive at the alpha-particle potential, the parameters of which are given in Table 1 for the relevant nuclei.

The imaginary part of the OP for alpha particles must be selected on the basis of the best agreement with absolute values of $\langle \Gamma_{\alpha} \rangle_{ex}$. Table 3 shows the results of such calculations with $W_0 = 2$ MeV, $R_{ow} = 1.215 A^{1/3}$ f and $a_w = 1.5$ f (the absorption has a Gaussian shape). The penetration factors necessary for obtaining the strength functions and for considering the statistical properties of the α -particle widths [1] were calculated using the method proposed in Ref. [4], taking as channel radius the position of the peak of the irregular scattering function g_{ℓ} in the real part of the alpha potential closest to the internal reversal point. Table 2 shows the strength functions in relation to A and E_{α} , the energy of the alpha transitions calculated from the optical model and obtained by experiment.

In accordance with the hypothesis as to the possible existence of giant resonances in the interaction of alpha particles with a nuclear substance, it should be assumed that all the measured nuclei reach a minimum between single-particle resonances.

REFERENCES

- [1] POPOV, Yu.P., JINR preprint EZ-5483, Dubna (1970).
- [2] KADMENSKY, S.G., KALEGITS, V.E., FURMAN, V.I., et al., Jademaja Fizika 10 (1969) 730.
- [3] FAYANS, A.S., Institute of Atomic Energy preprint IAE-1593 (1970).
- [4] VOGT, E., et al., Phys. Rev. 61 (1970) 864.

Table 1

Target nucleus	Product nucleus	$Z_{0V} \times 10^{-13}$ cm	$V_{0\alpha}$ MeV	Target nucleus	Product nucleus	$Z_{0V} \times 10^{-13}$ cm	$V_{0\alpha}$ MeV
Zn ⁶⁴	Ni ⁶¹	1.2010	201	Sm ¹⁴⁷	Nd ¹⁴⁴	1.2215	205
Zn ⁶⁷	Ni ⁶⁴	1.2018	201	Sm ¹⁴⁹	Nd ¹⁴⁵	1.2220	205
Mo ⁹⁵	Zr ⁹²	1.2075	203	Eu ¹⁵¹	Pm ¹⁴⁸	1.2223	205
Pd ¹⁰⁵	Ru ¹⁰²	1.2105	204	Gd ¹⁵⁵	Sm ¹⁵²	1.2227	205
Te ¹²³	Sn ¹²⁰	1.2175	204.5	Hf ¹⁷⁷	Yb ¹⁷⁴	1.2254	206
Nd ¹⁴³	Ce ¹⁴⁰	1.2210	205	Os ¹⁸⁷	W ¹⁸⁴	1.2264	206,5
Nd ¹⁴⁵	Ce ¹⁴²	1.2212	205	Os ¹⁸⁹	W ¹⁸⁶	1.2267	206,5

Table 2

Target nucleus	S_{α}^J	Permissible l_{α}	$\frac{N_{\alpha}^{J\pi}}{N^{J\pi}}$	$(S_{\alpha}^J)_{exp.} \times 10^2$	$(S_{\alpha}^J)_{om} \times 10^3$
Mo ⁹⁵	S_{20}^{2+}	2	3/3	0,12±0,1	0,33±0,08
Te ¹²³	S_{20}^{0+}	0	3/4	0,38±0,13	0,37±0,09
Nd ¹⁴³	S_{20}^{3-}	3	4/7	0,43±0,15	0,45±0,08
Nd ¹⁴⁵	S_{20}^{3-}	3	3/3	≤0,72±0,13	0,35±0,06
Sm ¹⁴⁷	S_{20}^{3-}	3	7/7	0,43±0,11	0,56±0,18
	S_{21}^{3-}	1, 3, 5	6/7	0,23±0,15	0,45±0,15
Sm ¹⁴⁹	S_{21}^{4-}	3, 5	4/4	0,27±0,12	0,45±0,15
	S_{20}^{3-}	3	6/7	<0,3 ±0,1	0,7 ±0,2

Table 3

Target nucleus	No. of widths N	$\langle D_H \rangle$ (eV)	$\langle \Gamma_{\alpha} \rangle_{\text{exp}}$ μeV	$\langle \Gamma_{\alpha} \rangle_{\text{CM}}$ μeV	$\frac{\langle \Gamma_{\alpha} \rangle_{\text{exp.}}}{\langle \Gamma_{\alpha} \rangle_{\text{CM}}}$
Zn^{64}	2/2	4300 \pm 800	$(2,4^{+2}_{-1,5}) \cdot 10^2$	$(0,84 \pm 0,17) \cdot 10^2$	$2,8^{+2,5}_{-2,0}$
Zn^{67}	1/2	700 \pm 250	$(8^{+8}_{-5}) \cdot 10^2$	$(57 \pm 20) \cdot 10^2$	$0,14^{+0,14}_{-0,1}$
Mo^{95}	6/6	80 \pm 20	11 ± 7	25 ± 6	$0,44 \pm 0,3$
Pu^{105*}	3/3	13 \pm 3	$\leq 1,3$	$1,05 \pm 0,24$	$\leq 1,25$
Te^{123}	6/6	30 \pm 7	$2 \pm 1,3$	$0,7 \pm 0,17$	$2,85 \pm 2$
Nd^{143}	8/13	38 \pm 6	8 ± 3	6 ± 1	$1,3 \pm 0,6$
Nd^{145*}	3/3	20 \pm 3	$2,6 \pm 0,7$	$1,65 \pm 0,3$	$1,6 \pm 0,7$
Sm^{147}	19/19	6,8 \pm 1,6	$2,3 \pm 0,7$	$4,0 \pm 1$	$0,58 \pm 0,25$
Sm^{149}	15/17	2,7 \pm 0,5	$0,19 \pm 0,04$	$0,37 \pm 0,1$	$0,52 \pm 0,2$
Eu^{151*}	11/1	0,85 \pm 0,14	$\geq 0,85 \cdot 10^{-4}$	$(1,3 \pm 0,25) \cdot 10^{-4}$	$\geq 0,65$
Gd^{153*}	11/1	2,0 \pm 0,4	$\geq 1,47 \cdot 10^{-4}$	$(9,2 \pm 2) \cdot 10^{-4}$	$\geq 0,16$
Hf^{177}	5/5	2,3 \pm 0,5	$(3 \pm 2) \cdot 10^{-3}$	$(14 \pm 3) \cdot 10^{-3}$	$0,22 \pm 0,16$
Os^{187}	2/2	10,4 \pm 2	$\leq 1,2$	$0,2 \pm 0,04$	≤ 6
Os^{189}	6/6	5,1 \pm 1	$\leq 0,23$	$0,18 \pm 0,03$	$\leq 1,25$

Remark: In the case of nuclei marked *, all the resonances studied have the same spin.

APPARATUS FOR INVESTIGATING THE (n, α) REACTION

Yu.P. Popov, K.G. Rodionov, R.F. Rumi, V.G. Semenov,
M. Stempinski, M. Florek

Using powerful neutron beams from pulsed sources, the authors consider various aspects of the recording and spectrometry of alpha particles and describe the characteristics of alpha-particle detectors, which have been developed by the group: a gas scintillation detector with electrical field, a multilayer ionization chamber with central collector, a multisection proportional chamber, and also alpha-ray spectrometers based on a multilayer ionization chamber and an ionization chamber with inclined target. The main characteristics of these detectors are indicated in the table.

Table 1

Type of detector	Target area, $[cm^2]$	Efficiency Natural with respect to alpha particles (n, α) in the reaction, [%]	background of the detector (pulses/h.cm ²) in the energy range (MeV)	Detector resolution for 4.5 MeV alpha-particle energy (keV)		The detectors and spectrometer are capable of operating with a neutron source pulse power of 60 MW without variation in the main characteristics, starting (usec) after a burst over the flight length (m)	
				Outside neutron beam	In neutron beam	[μ sec]	[m]
Gas scintillation detector	7000	30-40	0.012 (1.5-7)	-	-	300	100
Ionization chamber with central collector	4000	30-40	0.012 (7-12)	300	600	600	100
Multisection proportional chamber	13000	40	0.006 (1-10)	-	-	200	30
Double ionization chamber with slit collimator	1600	100	0.013 (5-10)	100	200-400	400	100
Large ionization chamber	9000	100	0.013 (5-10)	100	200-400	1200	100

INVESTIGATION OF NEUTRON RADIATIVE CAPTURE REACTIONS
LEADING TO SPONTANEOUSLY FISSIONABLE ISOMERS

Yu.P. Gangrsky, B.N. Markov, T. Nad,
I.F. Kharisov

The authors measured the cross-sections for the formation of the spontaneously fissionable isomers ^{236}U , ^{242}Am , ^{244}Am in the radiative capture of neutrons with energies of 1-3 MeV and of thermal neutrons. In the case of the isomers ^{242}Am and ^{244}Am with half-lives of 14 μsec and 1.1 msec respectively, a pulsed neutron beam was employed and the fission fragment yield was measured in the period between neutron pulses. In the case of the isomer ^{236}U with half-life 70 nsec the delayed coincidences of conversion electrons and fission fragments were measured during a continuous thermal neutron flux. The measured cross-sections for the formation of spontaneously fissionable isomers reveal a correlation with the induced fission cross-sections. This correlation is evidently a reflection of the complex structure of the fission barrier.

Table

Cross-sections for formation of spontaneously
fissionable isomers

Isomer	Neutron energy	Cross-section, mbarn
^{236}U	0,025 eV	~ 60
^{242}Am	0,025 eV	$0,3 \pm 0,1$
	1,0 MeV	$0,04 \pm 0,015$
	2,0 MeV	$0,03 \pm 0,01$
^{244}Am	0,025 eV	< 0,01
	1,0 MeV	$0,04 \pm 0,015$
	2,0 MeV	$0,025 \pm 0,008$
	3,0 MeV	$0,015 \pm 0,005$

ORIENTED TARGETS AND POLARIZED NEUTRONS
IN NEUTRON PHYSICS

V.P. Alfimenkov

On the basis of the relevant literature the author considers experiments that have been performed and possible future experiments involving polarized slow neutrons and oriented nuclear targets. Particular attention is devoted to measurement of the spin components of the cross-section for slow neutron interaction with nuclei, the determination of neutron resonance spins and determination of the magnetic and electric moments of excited nuclear states.

STUDY OF THE INTERACTION BETWEEN A NEUTRON AND
AN ELECTRON, MADE WITH THE PULSED FAST REACTOR
OF THE JOINT INSTITUTE OF NUCLEAR RESEARCH

Yu.A. Aleksandrov, A.M. Balagurov, A.I. Vasilenko
T.A. Machekhina, G.S. Samosvat

The time-of-flight method was used to measure the intensity of Bragg reflections from single crystals of tungsten enriched in ^{186}W . The isotopic compounds of the specimens were such that their total coherent scattering amplitudes were of different signs. A value of $a_{re} = (-1.32 \pm 0.11) \times 10^{-16}$ cm was obtained for the neutron-electron scattering amplitude. The prospects of further study in this direction are considered.

THE IBR-30 AND IBR-2 PULSED REACTORS WITH INJECTORS
AS SOURCES FOR NEUTRON SPECTROSCOPY IN THE
RESONANCE ENERGY REGION

Yu.S. Yazvitsky

This paper describes some features of the IBR-30 and IBR-2 pulsed reactors of the Joint Institute of Nuclear Research. The IBR-30 reactor was commissioned in 1969 and has a mean capacity of 25 kW. Construction of the IBR-2 reactor was commenced in 1969 and its mean rated capacity is 4 MW. The IBR-30 and IBR-2 reactors have linear electron accelerators as injectors and they can operate under boosted conditions.

Characteristics of the IBR-30 and IBR-2 reactors and their injectors are given in Tables 1 and 2. The number of neutrons in the 1-eV energy range bombarding an area of 1 cm^2 at a distance L_M from the reactor is given by the formulae:

For IBR-30 (experimental)

$$I = 2.7 \times 10^6 \frac{W}{E^{0.9} L^2}$$

For IBR-2 (theoretical)

$$I = 1.5 \times 10^6 \frac{W}{EL^2}$$

W is the capacity in kilowatts.

Under boosted conditions a power level of 2.5 kW is attained on IBR-30 with a frequency of 100 pulses/sec and $\vartheta_{\frac{1}{2}} \approx 3 \text{ } \mu\text{sec}$. The capacity of the IBR-2 under boosted conditions with $\vartheta_{\frac{1}{2}} > 1 \text{ } \mu\text{sec}$ is expressed by the formulae:

$$W = 1.4 \times 10^{-1} \vartheta_{\frac{1}{2}} \text{ MW}$$

Table 1

Characteristics of the IBR-30 and IBR-2 under normal reactor conditions

	IBR-30	IBR-2
Mean power level (kW)	25	4000
Pulse frequency (pulses/sec)	4-100	5-50
Mean neutron yield (pulses/sec)	1.3×10^{15}	1.8×10^{17}
Neutron lifetime (sec)	1.6×10^{-8}	4.2×10^{-8}
Power between pulses (kW)	1.2	220
Power at pulse peak with a frequency of 5 pulses/sec (MW)	120	8000
Neutron yield at pulse peak with a frequency of 5 pulses/sec	5.6×10^{18}	3.6×10^{20}
Pulse half-width (μsec)	70	90

Table 2

Characteristics of the injectors of the IBR-30
(LUE-40) and of the IBR-2 (LIU-30)

	LUE-40	LIU-30
Electron energy (MeV)	40	30
Electron current in a pulse (A)	0.2	250
Current pulse duration (μ sec)	1.6	0.5
Frequency (pulses/sec)	100	50

INSTITUTE OF EXPERIMENTAL AND THEORETICAL PHYSICS

THE NUCLEAR MAGNETIC RESONANCE OF BETA-ACTIVE ^8Li NUCLEI
FORMED IN POLARIZED NEUTRON CAPTURE
IN SINGLE CRYSTALS OF LiF

M.I. Bulgakov, A.D. Gulko, Yu.A. Oratovsky
S.S. Trostinin

(Paper submitted to Zh. éksp.teor. Fiz.)

Measurements were carried out at room temperature of the nuclear magnetic resonance of polarized beta-active ^8Li nuclei obtained in the capture of polarized thermal neutrons. Three single crystal LiF samples were used, oriented in the planes (100), (110) and (111) perpendicular to the magnetic field, and also two powdered samples of LiF and ^7LiF (with depleted ^6Li content). The shape of the peak was studied in terms of the resolution of the angular anisotropy of beta radiation of polarized ^8Li nuclei by a magnetic radiofrequency field H_I . Theoretical calculation of the shape of the peak was performed, assuming dipole-dipole interaction for a hard lattice. The secondary moments of the resonance peak were calculated. Comparison with experimental results shows that the internal local fields in the case of ^8Li nuclei have a Gaussian distribution which deviates towards the Lorentz shape only in the wings ($\sim 10^{-2}$ of the maximum value). The shape of the resonance peak did not seem to be significantly affected by lattice disturbances caused by gamma-recoils of ^8Li nuclei.

NUCLEAR RESEARCH INSTITUTE OF THE ACADEMY OF SCIENCES
OF THE UKRAINIAN SSR

THE USE OF TWO DETECTORS FOR MEASURING TOTAL
CROSS-SECTIONS IN THE THERMAL REGION

V.P. Vertebny, P.N. Vorona, A.I. Kalchenko,
V.K. Rudishin, V.A. Pshenichny, I.P. Stolyarevsky
N.A. Trofimova

(Paper presented at the Conference on
Neutron Physics, Kiev, May 1971)

The authors propose the use of two detectors with different path lengths for studying the effect of diffraction scattering of slow neutrons by grains. The following results were obtained for the energy dependence of the total cross-sections of osmium isotopes in the 0.07-0.3 eV energy range:

$$\text{for osmium-187 } \sigma_{tot} = 7.4 + \frac{7.04 \times 10^5}{v} / \text{barn}$$

$$\text{for osmium-190 } \sigma_{tot} = 17.8 + \frac{3.52 \times 10^4}{v} / \text{barn}$$

$$\text{for osmium-192 } \sigma_{tot} = 16.6 + \frac{2.42 \times 10^4}{v} / \text{barn}$$

The scattering cross-section for osmium-186, 187, 190, 192 and natural osmium, obtained by extrapolating σ_{tot} to $t = 0$ are, respectively: 18 ± 5 , 75 ± 6 , 18 ± 2 , 17 ± 1 and 15 ± 3 barn. The radiation capture cross-sections for these isotopes are 80 ± 13 , 320 ± 10 , 16 ± 5 and 11 ± 5 b. However, in view of the possibility of small angle scattering occurring with all isotopes, these figures give only the lower limit except for ^{187}Os . In the case of ytterbium-168 the total cross-section for $v = 2200$ m/sec is 4100 ± 700 b. The large cross-section is mainly due to the resonance of ^{168}Yb at $E = 0.6$; however, a negative level contribution was also observed.

DETERMINATION OF TOTAL CROSS-SECTIONS FOR THE
SCATTERING OF SLOW NEUTRONS BY ATOMIC NUCLEI

V.P. Vertebny, N.L. Gnidak, E.A. Pavlenko,
V.K. Rudishin

(Paper presented at the Conference on
Neutron Physics, Kiev, May 1971)

On the VVR-M reactor of the Nuclear Research Institute of the Academy of Sciences of the Ukrainian SSR the time-of-flight method was used to measure the total neutron scattering cross-sections for a number of isotopes in the 0.01-10 eV energy range. The resolution was 3-6 $\mu\text{sec/m}$. The measurements were performed with respect to vanadium, the scattering cross-section of which was taken to be 5.1 b.

The method of measurement is quite sophisticated. The detector consists of a battery of SNM-37 counters filled with helium-3 to a pressure of 7 atm. This makes it possible to increase the neutron recording efficiency to almost 100% and at the same time reduce corrections for variations in recording efficiency due to angular anisotropy of the scattered neutrons and variation in neutron energy during scattering. Methods have been developed for determining the background from the walls of the container for $n\sigma_t < 0.1$ and $n\sigma_t \geq 0.1$ (when using powders). Analytical formulae are given for correcting for multiple scattering and absorption of neutrons in the sample. Calculations using these formulae agree with calculations by the Monte Carlo method to within 2-3%.

The results of measurements of total cross-sections for scattering by metal foils made from natural holmium, erbium, ytterbium, dysprosium and thulium are given in the table, where E_n is neutron energy in eV; σ_3 is the total neutron scattering cross-section (without deduction of the magnetic scattering cross-section σ_M ; $\bar{\sigma}_3 \equiv \sigma_3 - \sigma_M$). By comparing the total cross-sections for neutron scattering by oxides and metals it can be deduced that the magnetic scattering of neutrons by the ions Er^{3+} , Ho^{3+} , Dy^{3+} , Yb^{3+} , Tm^{3+} is practically identical in oxides and metals.

Allowing for possible systematic errors, the authors recommend the following cross-sections for scattering of neutrons by atomic nuclei of holmium, ytterbium and thulium in the 0.02-1.4 eV energy interval: 12.4 ± 0.6 , 25.0 ± 0.6 and 12.0 ± 0.4 b respectively; and for erbium in the 0.02-0.12 eV energy interval: 11.0 ± 0.3 b.

Table

Cross-sections for neutron scattering by nuclei of holmium, dysprosium, ytterbium, thulium and erbium

E _n , eV	Ho		Dy		Yb		Tm		Er	
	$\bar{\sigma}_s$, barn	σ_s , barn	$\bar{\sigma}_s$, barn	σ_s , barn	$\bar{\sigma}_s$, barn	σ_s , barn	$\bar{\sigma}_s$, barn	σ_s , barn	$\bar{\sigma}_s$, barn	σ_s , barn
1,38	12,2 ± 1,0	12,8 ± 0,8	50,0 ± 10	50,0 ± 10	23,2±0,6	23,3±0,6	12,2 ± 0,8	12,3 ± 0,6		
0,62	12,0	13,4	59,7 ± 3	61,0 ± 3	26,0±0,6	26,2±0,5	11,8	12,2		
0,35	12,1	14,4	68,9	71,0	25,0	25,6	11,9	12,8		
0,22	12,1	15,1	73,7	76,5	25,2	25,8	12,1	13,3		
0,15	12,0	16,2	76,4	80,0	25,0	25,9	12,3	14,0		
0,12	12,0	17,3	78,9	84,0	25,2	26,1	12,1	14,8	11,0	15,0
0,09	12,8 ± 0,5	19,8 ± 0,3	78,5 ± 3	85,0 ± 2	25,0±0,4	26,2±0,4	12,2 ± 0,3	15,0 ± 0,3	10,8 ± 0,4	16,1 ± 0,4
0,07	13,0	22,0	79,7	88,0	25,1	26,6	12,0	16,2	10,8	17,7
0,055	12,4	23,4	80,0	90,0	24,7	26,6	12,0	16,4	11,2	18,7
0,05	12,2	25,2	81,2	93,2	24,5	26,7	12,0	17,0	10,9	20,6
0,04	13,0 ± 0,5	28,2 ± 0,3	82,3 ± 3	96,5 ± 3	24,8±0,4	27,4±0,4	12,1 ± 0,3	18,0 ± 0,3	10,8 ± 0,2	22,6 ± 0,2
0,032	12,9	30,9	83,2	99,5	24,6	27,6	11,9	18,7	11,2	24,3
0,028	12,0	33,5	83,6	102,0	24,4	28,2	11,9	19,4	11,0	26,5
0,0253	12,0 ± 0,6	37,0 ± 0,5	85,5 ± 4	106,0 ± 4	25,0 ± 0,6	28,9±0,5	12,1 ± 0,4	20,9 ± 0,3	11,0 ± 0,3	28,5 ± 0,3
0,020	12,9 ± 2,0	40,0 ± 1,0	90,0 ± 10	113,0 ± 6	24,6 ± 1,0	29,0±0,8	11,9 ± 0,8	23,5 ± 0,6	11,0 ± 0,5	30,0 ± 0,5

STUDY OF THE INTERACTION OF SLOW NEUTRONS WITH ISOTOPES
OF A NUMBER OF ELEMENTS IN THE MASS
NUMBER RANGE 168-192

V.P. Vertebny, P.N. Borona, A.I. Kalchenko, V.V. Koloty,
M.V. Pasechnik, V.A. Pshenichny, Zh.I. Pisanko, V.K. Rudishin

(Paper presented at the Conference on Neutron
Physics, Kiev, May 1971)

With the VVR-M reactor of the Nuclear Research Institute of the Academy of Sciences of the Ukrainian SSR measurements were made of the transmission of samples enriched in osmium-186, 187, 189, 190, 192 and ytterbium-168, using a resolution of ~ 50 nsec/m, for neutrons of energy less than 1000 eV. Table 1 shows the resonance parameters of the osmium isotopes and Table 2 shows the distances observed between levels $\bar{D} = \Sigma D_i/n$ and $D^* = (\frac{\pi}{4M} \Sigma D_i^2)^{1/2}$; Table 3 shows the strength functions $S^* = \frac{\Gamma_n^0}{D^*} \text{bm}$ and $S' = \frac{\Sigma \Gamma_n^0}{\Delta E} \text{bm}$ (most probable values). Table 4 shows the resonance parameters of ^{168}Yb (the measurements were carried out on a sample with 17.1% ^{168}Yb enrichment). The ^{168}Yb levels were identified using the results for ^{170}Yb given in BNL-325, Supplement No. 2 (1966). The mean distance between levels for ^{168}Yb was $\bar{D} = (4.5 \pm 1)$ eV and $D^* = (4.3 \pm 0.9)$ eV. Of interest here is the smallness of the ^{192}Os strength function compared with the other osmium isotopes. The distances between levels (referred to a nuclear excitation energy of 6.5 MeV and $D = 0$) of even-odd compound osmium nuclei come into the region of the minimum of the gross structure of D_0 as a function of N . For even-odd compound nuclei of ytterbium a dependence is observed in D_0 relative to N which is typical of the erbium, dysprosium and gadolinium isotope families.

Table 1

Levels of osmium isotopes

F	E_c, eV	Γ_n^0, meV	J^{π}	E_0, eV	Γ_n^0, meV
Osmium-186					
1.	$22,37 \pm 0,08$	$2,4 \pm 0,3$	4.	$89,5 \pm 0,7$	-
2.	$44,3 \pm 0,25$	$12,3 \pm 1$	5.	136 ± 1	~ 30
3.	$65,9 \pm 0,45$	$10,4 \pm 3,7$	6.	$274 \pm 4 (?)$	-
Osmium-188					
1.	$38,4 \pm 0,2$	$6,9 \pm 0,6$	5.	314 ± 5	-
2.	$44,3 \pm 0,25 (?)$	$0,48 \pm 0,16$	6.	332 ± 5	-
3.	$78,5 \pm 0,5$	52 ± 4	7.	386 ± 6	-
4.	187 ± 2	-			
Osmium-190					
1.	$11,14 \pm 0,03$	-	4.	$165 \pm 1,5$	-
2.	$90,8 \pm 0,7$	$\approx 2,6$	5.	$323 \pm 5 (?)$	~ 83
3.	144 ± 1	$\approx 7,5$	6.	563 ± 10	-
Osmium-192					
1.	$20,33 \pm 0,08$	$(1,7 \pm 0,5) \cdot 10^{-3}$	4.	523 ± 10	~ 25
2.	$126 \pm 1 (?)$	$0,40 \pm 0,04$	5.	585 ± 11	-
3.	241 ± 3	~ 16	6.	717 ± 16	~ 5

Table 1 (continued)

Osmium-187

$\#$	$E_0, \text{ eV}$	$2gfn^c, \text{ meV}$	$\#$	$E_0, \text{ eV}$	$2gfn^c, \text{ meV}$
1.	$9,46 \pm 0,02$	$0,28 \pm 0,06$	6.	$47,3 \pm 0,26$	$3,3 \pm 0,3$
2.	$12,70 \pm 0,03$	$3,84 \pm 0,06$	7.	$50,0 \pm 0,3$	$8,1 \pm 2,8$
3.	$20,19 \pm 0,07$	$0,56 \pm 0,05$	8.	$63,4 \pm 0,4$	10
4.	$40,4 \pm 0,2$	$4,4 \pm 0,6$	9.	$89,5 \pm 1,5$	-
5.	$43,4 \pm 0,22$	-	10.	124 ± 1	54 ± 9

Osmium-189

1.	$6,75 \pm 0,01$	$1,16 \pm 0,04$	11.	$41,2 \pm 0,2$	$0,10 \pm 0,08$
2.	$8,97 \pm 0,02$	$2,8 \pm 0,2$	12.	$43,0 \pm 0,2$	$0,24 \pm 0,05$
3.	$10,30 \pm 0,03$	$1,2 \pm 0,1$	13.	$50,0 \pm 0,3$	$4,5 \pm 0,4$
4.	$16,69 \pm 0,07$	$1,2 \pm 0,1$	14.	$54,13 \pm 0,3$	$3,8 \pm 0,6$
5.	$22,04 \pm 0,08$	$1,8 \pm 0,3$	15.	$60,3 \pm 0,4$	$0,88 \pm 0,14$
6.	$22,71 \pm 0,06 (?)$	-	16.	$64,2 \pm 0,4$	~ 10
7.	$27,48 \pm 0,1$	$1,0 \pm 0,2$	17.	$74,3 \pm 0,5$	-
8.	$28,18 \pm 0,12$	$3,8 \pm 1$	18.	$86,9 \pm 0,6$	-
9.	$30,18 \pm 0,12$	$0,19 \pm 0,02$	19.	$90,8 \pm 0,7 (?)$	-
10.	$38,4 \pm 0,2$	$0,47 \pm 0,08$	20.	$113 \pm 1,0$	-
$\#$	$E_0, \text{ eV}$	$\#$	$E_0, \text{ eV}$	$\#$	$E_0, \text{ eV}$
21.	108 ± 1	26.	$138 \pm 1,2$	31.	200 ± 2
22.	$112 \pm 1 (?)$	27.	$144 \pm 1,2$	32.	214 ± 3
23.	116 ± 1	28.	$155 \pm 1,5$	33.	235 ± 3
24.	$120 \pm 1,2 (?)$	29.	$161,5 \pm 1,5$	34.	260 ± 4
25.	$126 \pm 1,2$	30.	$172 \pm 2 (?)$	35.	$323 \pm 5 (?)$

Table 2

Mean distances between levels of osmium isotopes

ISOTOPE	\bar{D} (eV)	D^* (eV)	ISOTOPE	\bar{D} (eV)	D^* (eV)
I86	22 ± 6	22 ± 6	I87	$8 \pm 1,6$	$9 \pm 1,8$
I88	47 ± 10	57 ± 12	I89	$3,8 \pm 0,7$	$4,5 \pm 0,8$
I90	52 ± 14	52 ± 14			
I92	140 ± 35	144 ± 35			

Table 3

Strength functions of osmium isotopes

ISOTOPE	$S^* \times 10^4$	$S' \times 10^4$	ISOTOPE	$S^* \times 10^4$	$S' \times 10^4$
I86	$5,6^{+7,8}_{-2,3}$	$5,6^{+7,8}_{-2,3}$	I87	$2,0^{+2,0}_{-0,8}$	$2,4^{+2,4}_{-1,1}$
I88	$5^{+9}_{-2,5}$	$5^{+9}_{-2,5}$	I89	$2,0^{+1,0}_{-0,6}$	$2,2^{+1,1}_{-0,7}$
I92	$0,6^{+0,9}_{-0,2}$	$0,6^{+0,9}_{-0,2}$			

Table 4

Resonance parameters of ^{168}Yb

#	E_0 (eV)	Γ_n^0 (meV)	Γ_γ (meV)	#	E_0 (eV)
I.	$E_0 < 0$			II.	$78,5 \pm 0,5$
2.	$0,600 \pm 0,008$	$2,66 \pm 0,26$	90 ± 6	I2.	$80,7 \pm 0,6$
3.	$3,925 \pm 0,008$	$0,053 \pm 0,006$	75 ± 25	I3.	253 ± 4
4.	$8,17 \pm 0,03$	-	-	I4.	289 ± 4
5.	$9,74 \pm 0,03$	$0,05 \pm 0,02$	140 ± 30		
6.	$22,60 \pm 0,05$	$10,5 \pm 1,1$	-		
7.	$27,48 \pm 0,1$	$1 \pm 0,4$	-		
8.	$40,8 \pm 0,2$	-	-		
9.	$56,8 \pm 0,4(?)$	-	-		
10.	$66,8 \pm 0,4$	16 ± 2	-		

TOTAL NEUTRON CROSS-SECTIONS OF EUROPIUM,
GOLD AND WATER IN THE
0.008-0.3 eV ENERGY RANGE

V.P. Vertebyny, M.F. Vlasov, R.A. Zatserkovsky,
A.I. Ignatenko, A.L. Kirilyuk,
N.A. Trofimova, A.F. Fedorova

Using the VVR-M reactor of the Nuclear Research Institute of the Academy of Sciences of the Ukrainian SSR, the authors applied the time-of-flight method in measuring the total neutron cross-sections of europium-153 and natural europium, and the results were then used to calculate the cross-section of europium-151. The resolution was 3.5 μ sec/m. The ^{153}Eu sample was in the form of the oxide $^{153}\text{Eu}_2\text{O}_3$ with 99.3% enrichment and a thickness of 1.35×10^{21} nuclei/cm². It was shown experimentally that the contribution of highly absorbent impurities [Gd] to the σ_{tot} value of the sample amounts to $(5 \pm 3)\%$ and this was allowed for when calculating the total cross-section of europium-153.

For checking purposes the measurements of the total cross-section of natural europium were carried out on three types of samples:

- (1) High-purity Eu_2O_3 powder (total impurity of highly absorbent elements 10^{-5});
- (2) The same Eu_2O_3 powder mixed with graphite;
- (3) Europium nitrate solution in heavy water.

The cross-sections for powdered samples are 4-4.7% greater than cross-sections obtained with the liquid sample. These differences are due to the inhomogeneity of the powdered samples. Results obtained by statistical averaging over all the samples agree for all practical purposes with the results for the liquid sample.

Table 1 shows the total neutron cross-sections of europium-151, europium-153 and natural europium in relation to neutron energy. The reduced error includes the statistical error, which was $< 1\%$, the error due to uncertainty of the contribution of highly absorbent elements and also the inaccuracy in the determination of the sample concentrations. It should be noted that the cross-section of natural europium was determined with respect to the cross-section of water at 20°C (Table 2) which was determined using the measured thickness of the container. Table 2 also shows the total neutron cross-sections for gold measured in relation to neutron energy.

Table 1

Energy dependence of the total neutron cross-sections
of ^{151}Eu , ^{153}Eu and natural Eu

Neutron energy in eV	Total cross-section of ^{153}Eu in barns	Total cross-section of ^{151}Eu in barns	Total cross-section of natural europium in barns
0,3	63 ± 4	4770 ± 170	2310 ± 90
0,25	67	3260 ± 120	1590 ± 60
0,2	88	1950	970 ± 40
0,15	107	1660 ± 60	850 ± 30
0,1	134	2040 ± 70	1045 ± 35
0,09	146 ± 5	2230	1140
0,085	150	2420	1230
0,080	155	2590	1310
0,075	159	2700	1370
0,070	163	2950 ± 90	1500 ± 50
0,065	171	3260	1650
0,060	181	3520	1780
0,055	187	3953	1970
0,050	199	4483	2250
0,045	210 ± 7	5117	2560
0,040	225	5805	2850
0,035	239	6710 ± 200	2340 ± 70
0,030	262	7990	3960
0,0253	282 ± 9	9490 ± 290	4690 ± 140
0,020	313	11540 ± 360	5680 ± 170
0,019	318	12260	6040
0,018	334	12550	6260
0,017	346	13350 ± 410	6570 ± 200
0,016	358	13970 ± 440	6870 ± 210
0,015	364 ± 11	14670 ± 460	7210 ± 230
0,014	376	15250 ± 480	7600 ± 240
0,013	395	15990 ± 500	8020 ± 260
0,012	405 ± 13	17030 ± 560	8420 ± 280
0,011	429	18480 ± 680	9060 ± 340
0,010	452 ± 15	19590 ± 840	9620 ± 420

Table 2

Energy dependence of total neutron cross-sections of
gold and water

Neutron energy in eV	Total cross-section of gold in barns	Total cross-section of H ₂ O in barns
1	29,1	46 ± 1,5
0,3	38,4	53,5
0,25	40,5 ± 1,5	56,8
0,2	43,8	58,6
0,15	51,0	64
0,1	57,5	71,3
0,09	60,2	72,7
0,085	62,3	73,8
0,080	64,0	74,8 ± 1
0,075	65,5	75,5
0,070	66,8 ± 0,8	76,8
0,065	69,1	78,3
0,060	70,8	80
0,055	74,1	83,0
0,050	76,7	85,4
0,045	82	88,8
0,040	85,2	92,2 ± 2
0,035	90,2	96,9
0,030	96,6	103,1
0,0253	105,1 ± 0,5	110,0 ± 3
0,020	116,2	117,6 ± 3
0,019	119	120,1
0,018	121,7	118,1
0,017	125,6 ± 0,5	130,5
0,016	128	126,9
0,015	133	131,5
0,014	138	135,0
0,013	140	132
0,012	150	
0,011	155 ± 5	
0,010	162	

THE DENSITY OF THE LEVELS OF COMPOUND NUCLEI IN THE REGION
A = 130-200 AND OTHER NUCLEAR PROPERTIES

V.P. Vertebny, A.I. Kalchenko, M.V. Pasechnik

(Paper presented at the Conference on Neutron
Physics, Kiev, May 1971)

The following notation is used: \bar{D}_0 is the mean distance between levels referred to an excitation energy of 6.5 MeV and $J = 0$; \bar{D}_{obs} is the experimentally observed mean distance between neutron resonances; P_z is the proton pair interaction energy according to Cameron and Gilbert; B_N is the neutron binding energy of a compound nucleus and N is the number of neutrons.

It is shown that the results of calculations according to the formula

$$D_0(6.5 \text{ MeV}) = \bar{D}_{\text{obs}} (2J+1) \left(\frac{6.5 - P_z}{B_N - P_z} \right)^2 \exp \left[2 \sqrt{\alpha(B_N - P_z)} \left(1 - \sqrt{\frac{6.5 - P_z}{B_N - P_z}} \right) \right]$$

for the distances between levels (referred to an excitation energy of 6.5 MeV and $J = 0$) for even-odd compound nuclei in the range $A = 130-200$ in relation to N - the number of neutrons - display the following features:

- (1) There are gross structure maxima of D_0 at $N = 82, 126$ and in the region of $N \approx 100-110$ with minima at $N \approx 90$ and $N \approx 115$;
- (2) For each family of isotopes there is a characteristic isotopic dependence:

If $N < 90$, D_0 increases as $N = 82$ is approached;

If $N \gtrsim 115$, D_0 increases as $N = 126$ is approached.

In the interval $N=90-115$ each family has a maximum of D_0 at $N \approx 100-110$. There are correlations in the relationships between the number of neutrons and the mean distances between levels (irrespective of their nature) in the region of the Fermi level and D_0 165 MeV. Similar correlations are observed also in the proton and neutron pairing energies. These behaviour patterns agree with the well-known theoretical work of V.M. Strutinsky, who showed that the position of closed shells varies with deformation of the atomic nuclei. It is worth noting that the entropies determined in the experiment for a number of nuclei in the rare earth range are 20-30% greater than the theoretical values, if only single-particle degrees of freedom are taken into account.

CORRELATION AND ANTICORRELATION OF THE REDUCED PROBABILITIES
IN (n,γ) AND (d,p) REACTIONS FOR NUCLEI WITH A ≤ 81

I.F. Barchuk, G.V. Belykh, V.I. Golyshkin, A.V. Murzin,
A.F. Ogorodnik

(Paper presented at the Conference on Neutron
Physics, Kiev, 1971)

In Ref. [1] correlations were discovered between the reduced probabilities of El transitions in the thermal-neutron reaction (n,γ) and the proton groups from the p-levels in the (d,p) reaction for even-odd nuclei with 25 ≤ A ≤ 67.

According to theory in Ref. [2] this is explained by the presence of a mechanism involving direct capture of the S-neutron by the p-level of the nucleus. Systematic investigation of the El transitions in the (n,γ) reaction for nuclei with 67 ≤ A < 81 [3] has shown that in this range of nuclei the correlations become weaker, whilst for ⁶⁹Zn, ⁷¹Ge, ⁷³G and ⁸¹Se there are anticorrelations. The latter point to a thermal neutron capture mechanism differing from direct capture. It is assumed that there exists here a mechanism involving the formation of "input states" of the nucleon-phonon type. Ref. [4] reports an attempt to find a basis for this mechanism. Fig. 1 shows the dependence of the correlation coefficient on the atomic number of even-odd nuclei with 25 ≤ A ≤ 81. The shaded points correspond to data which the authors obtained [3] for the (n,γ) reaction.

The correlation coefficient was calculated on the basis of data from the literature for the (n,γ) and (d,p) reactions, using the formula

$$P = \frac{\sum_i (x_i - \bar{x})(y_i - \bar{y})}{\left[\sum_i (x_i - \bar{x})^2 \sum_i (y_i - \bar{y})^2 \right]^{\frac{1}{2}}}$$

where x represents the reduced probability of an El transition, which is proportional to I_γ/E_γ^3 , which is determined experimentally in the (n,γ) reaction: (I_γ is the intensity of the gamma peak, E_γ is the energy of the gamma peak) and y represents the reduced neutron width, which is proportional to the spectroscopic factor $S(2j_f + 1)$ which was experimentally determined in the (d,p) reaction [5].

REFERENCES

- [1] GROSHEV, L.V., DEMIDOV, A.M., *Jadernaja Fizika* 4 (1966) 785.
[2] LANE, A.M., LYNN, J.E., *Nucl. Phys.* 17 (1960) 563, 586.

- [3] BARCHUK, I.F., BAZAVOV, D.A., BELYKH, G.V., GOLYSHKIN, V.I.,
MURZIN, A.V., OGORODNIK, A.F., *Jadernaja Fizika* 11 (1970) 934.
BARCHUK, I.F., BAZAVOV, D.A., BELYKH, G.V., GOLYSHKIN, V.I.,
MURZIN, A.V., OGORODNIK, A.F., *Ukr. Fiz. Ž* 15 (1970) 245.
BARCHUK, I.F., BAZAVOV, D.A., BELYKH, G.V., GOLYSHKIN, V.I.,
MURZIN, A.V., OGORODNIK, A.F., *Izd. Akad. Nauk SSSR, Ser. fiz.*
34 (1970) 1775.
BARCHUK, I.F., BAZAVOV, D.A., BELYKH, G.V., GOLYSHKIN, V.I.,
MURZIN, A.V., OGORODNIK, A.F., *Ukr. Fiz. Ž* 15 (1970) 2071.
- [4] KNATKO, V.A., RUDAK, E.A., *Jadernaja Fizika* 13, 3 (1971) 521.
- [5] LUCKLAMA, H., ARCHER, N.P., KENNET, T.J., *Nucl. Phys.* A100 (1967)
33, 43.

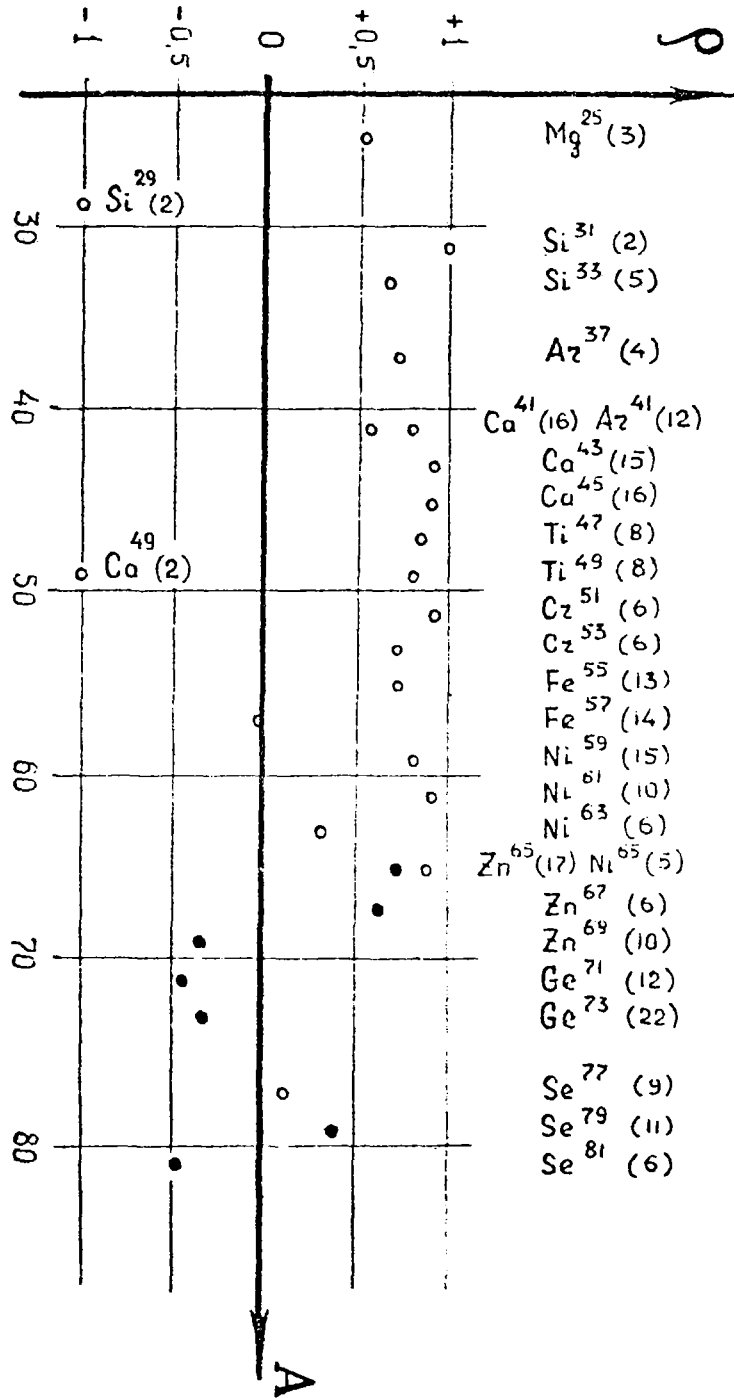


Fig. 1

ENERGY AND ISOTOPE-SPIN DEPENDENCE OF THE OPTICAL POTENTIAL
DERIVED FROM DATA ON NEUTRON SCATTERING

M.V. Pasechnik, I.A. Korzh, I.E. Kashuba

(Paper presented at the Conference on Neutron
Physics, Kiev, 1971)

This paper presents the results of an optical model analysis of data on the elastic scattering of polarized and non-polarized neutrons by nuclei in the mass number range $48 < A < 137$ for four neutron energies in the range 1.5-6.1 MeV. For calculating the total and differential cross-sections as well as the polarizing capacities of the nuclei the authors employed a local optical potential which takes into account the surface absorption and spin-orbital interaction. The optimum sets of potential parameters (V_c , W_c , V_{so} , a) were obtained by fitting the computed data to the experimental data using the method of least squares. The parameters r_0 and b were taken as constant:

$$r_0 = 1.25 \text{ f, and } b = 0.98 \text{ f.}$$

For each of the neutron energies investigated (1.5 MeV [1], 3.2 MeV [2], 4 MeV [3], 6.1 MeV) the best parameters were determined for all the nuclei concerned. The potential parameters corresponding to the best fits for neutron energy 6.1 MeV are given in Table 1. By averaging the parameters obtained for this energy, it was possible to obtain the optical potential parameters independent of mass. The averaged potential parameters were used for determining the energy dependence of the parameters. The averaged parameters V_{so} and a , which are practically independent of neutron energy, are 7.5 MeV and 0.65 f respectively. The real and imaginary parts of the central potential in the neutron energy range investigated are described by the equations:

$$V_c = (48.7 - 0.33 E) \text{ MeV}$$
$$W_c = (7.2 + 0.66 E) \text{ MeV}$$

Optical model analysis of our data on the scattering of polarized neutrons with energies of 1.5 MeV by medium nuclei enables us to establish the dependence of the real part of the central potential on the symmetry parameter $\alpha = (N - Z)/A$ as:

$$V_c = (51.8 - 30 \alpha) \text{ MeV}$$

The energy and isotope-spin relationships obtained for the real part of the central potential are in good agreement with the data of other authors (see Table 2).

REFERENCES

- [1] KORZH, I.A., et al., Programme and abstracts of papers for the XXI Annual Conf. on Nuclear Spectroscopy and the Structure of the Atomic Nucleus, Part 2, Leningrad (1971) 102.
KORZH, I.A., et al., Izv. Akad. Nauk SSSR, Ser. fiz. 35 (1971) 823.
KORZH, I.A., et al., Jadernaja Fizika 7 (1968) 277.
- [2] KASHUBA, I.E., KORZH, I.A., Ukr. fiz. Ž 15 (1970) 1036.
- [3] KASHUBA, I.E., KOZIN, B.D., Ukr. fiz. Ž 13 (1968) 51.
- [4] HOLMGVIST, B., Ark. Fys. 38 (1968) 403.
- [5] PEREY, F., BUCK, B., Nucl. Phys., 32 (1962) 353.
- [6] BJORKLUND, F., FERNBACH, S., Phys. Rev., 109 (1958) 1295.
- [7] ROSEN, L., et al., Ann. Phys., 34 (1965) 96.
- [8] CASSOLA, R.L., KOSCHEL, R.D., Nuovo Cim., B53 (1968) 363.

Table 1

Optimum values of the optical model parameters obtained from three-parameter analyses of data on the scattering of 6.1 MeV neutrons by medium nuclei. Comparison of the computed and experimental total cross-sections [4]

Element	V_c MeV	W_c MeV	a_1 fermi	$G_{\pm}^{comp.}$ barn	G_{\pm}^{ex} barn
V	48,0	9,5	0,66	3,392	3,51 ± 0,07
Cz	46,5	10,0	0,73	3,552	3,66 ± 0,08
Mn	47,5	10,0	0,67	3,553	3,62 ± 0,08
Co	47,0	11,0	0,69	3,689	3,74 ± 0,07
Ni	46,5	13,0	0,74	3,693	3,74 ± 0,07
Cu	46,5	12,5	0,74	3,826	3,84 ± 0,05
Zn	46,5	13,0	0,73	3,798	3,85 ± 0,07

Table 2

Comparison of the energy dependences of the real part of the central potential obtained by different authors

Range of neutron energies covered	Energy dependence	Literature references
I ÷ 25 MeV	48 - 0,29 E	(5)
4,1 ÷ 14 MeV	48 - 0,3 E	(6)
0,2 ÷ 24 MeV	49,3- 0,33 E	(7)
6 ÷ 24 MeV	48 - 0,35 E	(8)
1,5 ÷ 6,1 MeV	48,7- 0,33 E	

Data of this paper.

STUDY OF POLARIZATION IN THE ELASTIC SCATTERING OF
1.5 MeV NEUTRONS BY MEDIUM NUCLEI

I.A. Korzh, T.A. Kostyuk, V.A. Mishchenko, M.V. Pasechnik
N.M. Pravdivy, I.E. Sanzhur

(Paper presented at the Conference on Neutron
Physics, Kiev, 1971)

The polarizing capacities of nuclei of Ti, Cr, Fe, Co, Ni, Cu, Zn, Ge, Zr, Nb, Mo, Cd, Sn and Sb were determined for neutrons of energy 1.5 MeV in the $20-145^\circ$ angle range from measurements of right-left asymmetry in the scattering of partially polarized neutrons, produced by the reaction $T(p,n)^3\text{He}$ ($P_2(30^\circ) = 36 \pm 2\%$). The differential elastic scattering cross-sections of non-polarized neutrons were determined as the half sums of the cross-sections for scattering through the corresponding angles to the right and left of the bombarding neutron flux direction. The results of the measurements were corrected for neutron flux attenuation in the sample, finite geometry and multiple scattering.

The differential cross-sections are represented in the form of a Legendre polynomial expansion: $\sigma(\vartheta) \sum_{\ell=0}^{\infty} A_\ell P_\ell(\cos \vartheta)$. On the basis of measurements of $\sigma(\vartheta)$ the authors determined the total elastic scattering cross-sections σ_{el} , the transport cross-sections σ_{trel} and the mean values of the cosine of the elastic scattering angle, $\cos \vartheta$. The values of the calculated constants and the coefficients A_ℓ are given in Table 1. Data on the polarizing capacities of Ge, Cd, Sn and Sb nuclei are given in Table 2. Data on Ti, Cr, Fe, Co, Ni, Cu, Zn, Zr, Nb and Mo nuclei are contained in Ref. [1].

Experimental data on the angular distributions and the polarizing capacities of the investigated nuclei are analysed on the optical model. Theoretical calculations are performed using a six-parameter potential as proposed by Bjorklund and Fernbach.

REFERENCES

- [1] KORZH, I.A., et al., in Abstract Bulletin - Jaderno-Fizičeskie issledovanija v SSSR (Nuclear Physics Research in the USSR), Issue No. 10, Atomizdat (1970).

Table 1

Element	A_0	A_1	A_2	A_3	A_4	A_5	$G_{el.}$ barn	G_{total} barn	$\overline{\cos^2 \theta}$
Ge	0,181±0,002	0,237±0,007	0,222±0,008	0,146±0,012	0,059±0,011	0,014±0,011	2,273±0,045	1,282±0,064	0,436±0,017
Cd	0,382±0,009	0,561±0,022	0,574±0,027	0,190±0,033	0,113±0,026	0,010±0,031	4,798±0,096	2,447±0,108	0,490±0,020
Sn	0,471±0,003	0,621±0,006	0,645±0,009	0,168±0,011	0,156±0,010	0,032±0,014	5,916±0,136	3,319±0,140	0,439±0,020
Sb	0,382±0,002	0,603±0,005	0,591±0,006	0,217±0,010	0,066±0,008	0,025±0,009	4,798±0,082	2,274±0,125	0,526±0,018

Table 2

θ °	$P_2(\theta)$				
	l.s.c.*	Ge	Cd	Sn	Sb
20°		-0,061 ± 0,051	-0,043 ± 0,030	-0,041 ± 0,029	-0,069 ± 0,033
30°		-0,072 ± 0,045	-0,057 ± 0,038	+0,001 ± 0,043	-0,046 ± 0,024
40°		-0,059 ± 0,036	-0,074 ± 0,030	-0,035 ± 0,033	-0,045 ± 0,026
55°		-0,068 ± 0,050	-0,035 ± 0,041	+0,001 ± 0,032	-0,015 ± 0,033
70°		-0,018 ± 0,044	-0,104 ± 0,054	+0,006 ± 0,045	-0,033 ± 0,039
85°		+0,015 ± 0,039	-0,137 ± 0,061	-0,078 ± 0,067	-0,021 ± 0,046
100°		-0,032 ± 0,049	-0,165 ± 0,062	-0,135 ± 0,062	+0,012 ± 0,060
115°		-0,015 ± 0,068	-0,058 ± 0,081	-0,007 ± 0,080	+0,150 ± 0,072
130°		+0,048 ± 0,060	+0,148 ± 0,067	+0,092 ± 0,058	+0,203 ± 0,055
145°		+0,057 ± 0,053	+0,206 ± 0,063	+0,179 ± 0,046	+0,163 ± 0,048

* Laboratory system of co-ordinates.

ANALYSIS OF DATA ON THE SCATTERING OF 2.9 MeV NEUTRONS
BY NICKEL ISOTOPEs

M.B. Fedorov, T.I. Yakovenko

(Paper presented at the Conference on Neutron
Physics, Kiev, 1971)

The time-of-flight method was used to investigate the neutron spectrum resulting from elastic and inelastic scattering by the even-even isotopes ^{58}Ni , ^{60}Ni and ^{62}Ni with excitation of the lowest levels 2+ for an incident neutron energy of 2.9 MeV.

The differential cross-sections of elastically scattered neutrons are given in Table 1 (mb/sr).

Table 1

$\cos \theta$	Ni^{58}	Ni^{60}	Ni^{62}
0,87	527 ± 30	412 ± 32	596 ± 30
0,71	202 ± 27	174 ± 22	378 ± 30
0,50	80 ± 25	79 ± 16	148 ± 28
0,26	40 ± 12	31 ± 9	55 ± 17
0,00	39 ± 12	74 ± 15	43 ± 12
-0,26	205 ± 14	97 ± 14	146 ± 15
-0,50	101 ± 15	94 ± 13	158 ± 16
-0,71	97 ± 15	110 ± 15	102 ± 14

Table 2 shows the differential cross-sections of inelastic scattering with excitation of the lowest levels of the nickel isotopes (mb/sr).

Table 2

$\cos \theta$	Ni^{58}	Ni^{60}	Ni^{62}
0,87	51 ± 3	39 ± 3	39 ± 3
0,50	51 ± 3	42 ± 3	50 ± 3
0,26	44 ± 3	41 ± 3	44 ± 4
0,00	42 ± 3	45 ± 3	45 ± 3
-0,26	45 ± 3	40 ± 3	50 ± 3
-0,50	53 ± 3	40 ± 3	42 ± 3
-0,71	52 ± 3	41 ± 3	35 ± 4

The results are comparable with optical model calculations in accordance with the statistical theory of Hauser, Feshbach and Moldauer.

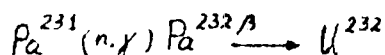
THE V.G. KHLOPIN RADIUM INSTITUTE OF THE ACADEMY OF
SCIENCES OF THE USSR

SLOW NEUTRON CAPTURE CROSS-SECTION FOR ^{231}Pa

B.M. Aleksandrov, M.A. Bak, A.S. Krivokhatsky, E.A. Shlyamin

(Article submitted to *Atomnaja Energija*)

Irradiation of ^{231}Pa in the reactor results in accumulation of ^{232}U according to scheme:



Since the ratio of periods of alpha-decay of the initial ^{231}Pa and the final ^{232}U is quite high ($\frac{T_{231}\text{Pa}}{T_{232}\text{U}} = 439$), a noticeable increase in the alpha activity of the target occurs ^{232}U during short irradiations of a few hours in a flux of $\sim 10^{14}$ n/cm² sec. The slow neutron capture cross-section for $^{231}\text{Pa}(\sigma_c)$, the integral neutron flux and the increase in the alpha activity of irradiated and cooled (for $\sim 10T_{232}\text{Pa}$) ^{231}Pa are associated with the relation:

$$\sigma_c = \frac{1}{\varphi t} \cdot \frac{I_{\text{U}^{232}}}{T_{\text{Pa}^{231}}} \left[\left(\frac{S_{\text{U}^{232}}}{S_{\text{Pa}^{231}}} \right)_{\text{without Cd}} - \left(\frac{S_{\text{U}^{232}}}{S_{\text{Pa}^{231}}} \right)_{\text{with Cd}} \right],$$

where φ is the neutron flux density;

t is the irradiation time;

$S_{232\text{U}}$ and $S_{231\text{Pa}}$ are the areas of the alpha peaks of ^{232}U and ^{231}Pa in the irradiation of cadmium-plated and plain targets.

The neutron flux at the location of the samples was measured using ^{237}Np targets.

The alpha spectra of irradiated and cooled targets with ^{231}Pa were measured on an alpha spectrometer with a surface-barrier gold-silicon detector. Since the relative measurements of the areas of the alpha peaks can be performed with an error of $\sim 1\%$, the main part of the measuring error of $\sigma_c(^{231}\text{Pa})$ is due to the measuring error of the neutron flux density and amounts to 4% .

As a result, the thermal neutron capture cross-section for ^{231}Pa was found to be 260 ± 13 b and the resonance capture integral (I_c) 1180 ± 120 b, the resonance capture integral for neptunium being taken as 945 b.

EXCITATION FUNCTIONS OF THE REACTIONS $^{27}\text{Al}(n,p)^{27}\text{Mg}$ AND $^{27}\text{Al}(n,\alpha)^{24}\text{Na}$

Yu.A. Nemilov, Yu.N. Trofimov

The sample activation method was used to measure the excitation functions of the reactions $^{27}\text{Al}(n,p)^{27}\text{Mg}$ and $^{27}\text{Al}(n,\alpha)^{24}\text{Na}$ in the neutron energy range 7.7-9.3 MeV. The reaction $^2\text{H}(\alpha,n)^3\text{He}$ was used to obtain monochromatic neutrons.

EXPERIMENTAL METHODS OF DETERMINING $\bar{\nu}(^{252}\text{Cf})$

K.A. Petrzhak, E.A. Shlyamin

(Paper presented at the Conference on Neutron Physics, Kiev, 1971)

On the basis of foreign literature a survey is made of experimental work in the past 10 years on absolute methods of determining $\bar{\nu}(^{252}\text{Cf})$. The 2% disagreement which exists in the results can not as yet be explained by systematic errors in one or another experiment. The summarized experimental results, corrected according to Hanna and Westcott [1], the weighted mean value and also the fitted value for $\bar{\nu}(^{252}\text{Cf})$ are shown in Table 1.

Table 1

Mean total number of neutrons per fission for ^{252}Cf

Authors	Method of measurement	Experimental values of $\bar{\nu}(^{252}\text{Cf})$ with Hanna correction
Asplund-Nilsson et al. [2]	Liquid spin-p	3.830 ± 0.037
Hopkins, Diven [3]	Liquid spin-p	3.793 ± 0.031
Colvin, Sowerby [4]	"BORON" reactor	3.713 ± 0.015
Moat et al. [5]	Mn-bath	3.727 ± 0.056
Colvin et al. [6]	Mn-bath	3.700 ± 0.031
White and Axton [7]	Mn-bath	3.796 ± 0.031
Axton [8]	Mn-bath	3.700 ± 0.020
De Volpi, Porges [9]	Mn-bath	3.739 ± 0.017
Weighted mean value		3.743 ± 0.016
Fitted value		3.7653 ± 0.0104

REFERENCES

- [1] HANNA, G.C., WESTCOTT, C.H., LEMMEL, H.D., LEONARD, B.R., STORY, G.S., ATTREE, P.M., Atom. Energy Rev. 7, 4 (1969) 3.
- [2] ASPLUND-NILSSON, J., CONDE, H., STARFELT, N., Nucl. Sci. Engng. 16, (1963) 124.
- [3] HOPKINS, J.C., DIVEN, B.G., Nucl. Phys. 48 (1963) 433.
- [4] COLVIN, D.W., SOWERBY, M.G., Physics and Chemistry of Fission 2, IAEA, Vienna (1965) 25.
- [5] MOAT, A., MATHER, D.S., McTAGGART, M.H., J. Nucl. Energy A/B, 15, (1961) 102.
- [6] COLVIN, D.W., SOWERBY, M.G., MacDONALD, R.I., Nuclear Data for Reactors 1, IAEA, Vienna (1967) 307.
- [7] WHITE, P.H., AXTON, E.J., J. Nucl. Energy, 22, (1968) 73.
- [8] AXTON, E.J., BARDELL, A.G., AUDRIC, B.N., EANDC(UK)-110(1969).
- [9] DE VOLPI, A., PORGES, K.G., Nuclear Data for Reactors, 1, IAEA, Vienna (1967) 297.

PROMPT NEUTRONS AND KINETIC ENERGY OF FRAGMENTS
FROM SPONTANEOUS FISSION OF ^{244}Cm

I.D. Alkhazov, S.S. Kovalenko, O.I. Kostochkin, L.Z. Malkin,
K.A. Petrzhak, V.I. Shpakov

(Article submitted to Jadernaya Fizika)

The authors measured the total number of prompt neutrons and the kinetic energy of both fragments for the spontaneous fission of ^{244}Cm in one fission event. This made it possible to obtain the dependence of the mean number of prompt neutrons per fission on the type of fission, as determined by the total kinetic energy and the mass of a heavy fragment. The number of neutrons in a fission event was measured using a liquid scintillation counter with an efficiency of 0.571 ± 0.011 , which was determined from the mean number (known from the literature) of prompt neutrons $\bar{\nu}$ in the spontaneous fission of ^{244}Cm [1, 2]. The fragment energies were measured with semiconductor detectors. The calibration and processing of the energy measurements are described in Ref. [3].

The measurements of neutrons from spontaneous fission of ^{244}Cm are recorded in Table 1. The accuracy of the data supplied is determined by the measuring statistics and the known accuracy of the neutron counter efficiency, which depends on the error in the literature data for $\bar{\nu}$ from spontaneous fission of ^{244}Cm (it was assumed that $\bar{\nu} = 2.78 \pm 0.05$ after recalibration with a more accurate value of $\bar{\nu}$ for spontaneous fission of ^{252}Cf) than that supplied in Refs [1, 2].

The slight errors introduced when correcting for counting errors due to coincidence of neutron pulses and for the background of the neutron counter (0.10 ± 0.01) were not taken into account. No corrections were introduced to cover variations in the neutron data due to energy dispersion during the measurements. The table shows the mean numbers of prompt neutrons per fission as a function of the total kinetic fragment energy and the mass of the heavy fragment. The latter data provided a means of calculating the relationship between the excitation energy consumed in neutron escape and the mass of the heavy fragment (Table 2). The mean fragment excitation energy associated with the escape of one neutron was determined as 7.2 ± 1.0 MeV.

REFERENCES

- [1] DIVEN, B.C., MARTIN, H.C., TASHEK, R.F., TERRELL, G., Phys. Rev. 101, (1956) 1016.
- [2] HICKS, D.A., ISE, J., PILE, R.V., Phys. Rev. 101 (1956) 1016.
- [3] ALKHAZOV, I.D., KOSTOCHKIN, O.I., KOVALENKO, S.S., MALKIN, L.Z., PETRZHAK, K.A., SHPAKOV, V.I., Jadernaja Fizika 11 (1970) 501.

Table 1

Mean number of prompt neutrons per fission $\bar{\nu}$ for spontaneous fission of ^{244}Cm
 as a function of total kinetic fragment energy E_K and heavy fragment mass M

$E_K \backslash M$	122	124	126	128	130	132	134	136	138	140	142	144	146	148	150	152	154	156	158	160	162	$\bar{\nu}(E_K)$
220	1,56	0,36	1,13	1,59	1,96	1,00	0,39	1,14														1,08
218	1,84	1,01	1,25	1,68	1,88	1,38	0,70	1,35														1,14
216	1,68	1,09	1,61	1,77	1,39	1,27	1,14	1,41														1,15
214	1,40	1,34	2,23	1,92	1,23	1,21	1,04	0,85	0,42	0,26												1,08
212	1,56	1,77	2,20	1,66	1,42	1,38	1,12	0,81	0,62	0,60	0,34											1,19
210	2,33	2,36	2,10	1,60	1,50	1,62	1,32	1,10	1,06	0,76	0,18											1,33
208	1,96	2,58	2,19	1,76	1,72	1,69	1,48	1,23	1,13	1,06	0,28	0,16										1,44
206	2,04	2,36	2,23	1,76	1,86	1,79	1,63	1,44	1,26	1,19	0,60	0,78										1,60
204	1,86	2,36	2,38	2,04	1,96	1,89	1,71	1,60	1,48	1,32	1,05	0,90										1,72
202	1,94	2,22	2,34	2,19	2,08	2,02	1,91	1,75	1,70	1,46	1,19	1,08	1,08									1,85
200	1,72	2,19	2,06	2,19	2,27	2,18	2,09	1,89	1,84	1,69	1,41	1,17	1,24	1,23								1,97
198	2,25	2,30	2,13	2,22	2,37	2,35	2,25	2,10	2,03	1,86	1,58	1,39	1,30	1,26	1,32							2,09
196	2,43	2,37	2,43	2,34	2,36	2,46	2,39	2,29	2,17	2,02	1,66	1,54	1,44	1,21	1,46							2,20
194	2,56	2,53	2,78	2,45	2,49	2,62	2,64	2,49	2,33	2,20	1,91	1,72	1,55	1,65	1,58	1,53						2,35
192	2,91	2,54	2,79	2,76	2,66	2,76	2,80	2,65	2,54	2,40	2,07	1,88	1,92	2,12	1,82	1,32	0,85					2,49
190	2,50	2,66	2,88	3,08	2,88	2,90	2,89	2,75	2,70	2,57	2,35	2,01	2,20	2,12	1,87	1,32	0,59	2,31				2,62
188	1,92	2,54	2,97	3,04	3,05	3,06	2,95	2,86	2,78	2,67	2,57	2,33	2,35	2,09	1,87	1,63	0,88	2,42	2,42			2,72
186	2,36	2,66	3,18	2,95	3,17	3,19	3,01	2,98	2,96	2,85	2,78	2,47	2,36	2,18	1,83	1,72	1,60	1,69				2,82
184	2,31	2,60	2,93	3,00	3,26	3,28	3,13	3,07	3,19	3,02	2,89	2,70	2,44	2,34	2,12	2,02	2,09	1,91	1,86			2,93
182	2,49	2,66	2,78	3,00	3,25	3,40	3,35	3,21	3,26	3,14	2,99	2,82	2,62	2,47	2,29	2,32	2,14	2,01	1,83	1,00		3,04
180	2,50	2,72	3,05	3,15	3,25	3,48	3,48	3,44	3,45	3,24	3,03	2,96	2,79	2,70	2,57	2,57	2,22	2,11	2,05	0,60	1,69	3,15
178	2,69	2,90	3,22	3,21	3,34	3,58	3,63	3,60	3,59	3,49	3,14	3,11	3,00	3,00	2,80	2,75	2,60	2,36	2,27	2,01	2,34	3,26
176	2,50	2,90	3,13	3,33	3,41	3,72	3,78	3,65	3,69	3,50	3,32	3,32	3,10	3,00	2,82	2,82	2,70	2,52	2,55	2,42	2,35	3,32
174	2,54	2,83	2,88	3,28	3,48	3,82	3,93	3,75	3,70	3,46	3,49	3,46	3,17	3,12	3,02	2,97	2,84	2,65	2,46	2,50	1,95	3,40
172	2,37	2,81	2,86	3,18	3,37	3,68	3,86	3,72	3,71	3,58	3,64	3,61	3,34	3,26	3,19	3,19	3,20	2,87	2,55	2,42	1,62	3,45
170	2,71	2,73	2,47	3,04	3,25	3,38	3,64	3,74	3,87	3,71	3,77	3,74	3,37	3,39	3,40	3,38	3,34	3,03	2,60	2,53	2,42	3,47
168	3,12	2,92	2,95	3,17	3,29	3,35	3,43	3,76	3,77	3,74	3,89	3,80	3,48	3,48	3,40	3,42	3,37	2,92	2,67	2,44	2,55	3,48
166	2,95	3,06	3,30	3,35	3,63	3,61	3,68	3,86	3,55	3,63	3,76	4,06	3,73	3,48	3,22	3,42	3,36	2,79	2,82	2,69	2,22	3,46

Table 1 (continued)

I	2	3	4	5	6	7	8	9	10	11	12	13	14	15	16	17	18	19	20	21	22	23
I64	2,63	2,97	3,16	3,00	3,73	3,79	3,65	3,80	3,71	3,76	3,82	3,96	3,96	3,47	3,52	3,47	3,48	3,20	2,82	2,84	2,44	3,49
I62	2,86	3,08	3,28	3,34	3,56	3,74	3,80	3,87	3,89	3,95	3,89	3,81	3,80	3,48	3,53	3,52	3,44	3,42	3,16	2,90	3,12	3,55
I60	2,81	2,90	3,20	3,56	3,47	3,48	3,86	3,60	3,62	4,12	3,90	3,77	3,84	3,74	3,87	3,74	3,60	3,38	3,48	3,32	3,57	3,57
I58	2,77	2,74	3,11	3,24	3,39	3,09	3,34	3,17	3,36	3,81	3,87	3,74	3,81	3,62	3,93	3,96	3,88	3,60	3,51	3,35	3,54	3,55
I56	2,65	2,98	3,15	2,80	2,87	2,82	3,10	3,13	3,36	3,90	3,99	3,48	3,77	3,75	3,87	3,94	3,82	3,60	3,37	3,16	3,50	3,45
I54	3,29	3,46	3,59	3,10	2,74	2,98	3,12	3,06	3,55	3,83	4,12	3,93	4,02	3,68	3,87	3,92	3,86	3,46	3,23	3,18	3,18	3,43
I52	3,43	3,36	3,36	3,09	2,91	2,93	2,94	3,16	4,16	3,63	3,79	3,99	3,77	3,28	3,80	3,95	4,6	3,67	3,23	3,27	3,25	3,45
$\bar{v}(M)$	2,62	2,72	2,78	2,71	2,69	2,71	2,74	2,70	2,74	2,71	2,67	2,70	2,79	2,87	2,93	2,95	3,04	3,04	3,01	2,90	2,91	2,78

Table 2

Excitation energy per fission consumed on neutron escape E_{xn}
in relation to heavy fragment mass M

M	126	128	130	132	134	136	138	140	142	144	146	148	150	152	154	156	158	160
E_{xn}	22,2	21,7	21,5	21,1	20,6	20,2	19,7	19,0	18,6	17,1	17,3	18,1	19,2	19,3	20,5	21,3	21,1	20,7

Table 3

Root mean square errors $\Delta v(E_K, M)$, Δv_{EK} and Δv_M for data of Table 1

$E_K \backslash M$	I24	I30	I40	I50	I60	$\Delta \sqrt{E_K}$
220		1,48				0,47
210	1,41	0,23				0,15
200	0,64	0,19	0,14			0,08
190	0,59	0,22	0,14	0,44		0,08
180	0,61	0,35	0,19	0,30		0,10
170	0,65	0,55	0,35	0,33	0,79	0,20
160	0,78	0,85	0,78	0,66	1,0	0,26
150	1,27	1,27	1,20	0,98	1,27	0,40
Δv_M	0,20	0,12	0,09	0,19	0,65	

MEASUREMENT OF THE MEAN KINETIC ENERGIES OF FRAGMENTS OF THE
FISSIONABLE NUCLEI ^{238}Pu , ^{239}Pu AND ^{240}Pu

V.A. Nikolaev

(Paper presented at the Conference on Neutron
Physics, Kiev, 1971)

Relative measurements were made of the mean kinetic energies of fragments of the fissionable nuclei ^{238}Pu , ^{239}Pu and ^{240}Pu produced during neutron-induced fission of ^{238}Pu and ^{239}Pu and by spontaneous fission of ^{238}Pu . The experiments involved the use of reactor neutrons and also monochromatic fast neutrons of energy 1100 ± 80 keV. The mean kinetic energies of the fragments were determined by measuring the diameters of the tracks of fragments slowed down in glass [1], using a calibration curve constructed on the basis of data for well-known isotopes. It is shown that the total kinetic energies of fragments of the fissionable nuclei ^{239}Pu and ^{240}Pu coincide within the error limits, whilst for the corresponding energies in the case of ^{238}Pu and ^{240}Pu there is a deviation of 5.5 ± 3 MeV out of line with the trend for the total kinetic energy to be proportional to the parameter $Z^2/A^{1/3}$.

REFERENCES

[1] GROMOV, A.V., NIKOLAEV, V.A., *Pribery Tekh. Eksp.*, 1 (1970) 245.

ANGULAR ANISOTROPY IN THE FISSION OF ^{226}Ra BY NEUTRONS
WITH ENERGIES OF 4-10 MeV

V.T. Ippolitov, Yu.A. Nemilov, Yu.A. Selitsky,
V.B. Funshtein

(Paper submitted to *Jadernaja Fizika*)

The authors have studied the fission of ^{226}Ra by neutrons in the 4-10 MeV range. The measurements carried out complement similar measurements reported earlier [1]. The angular distributions of fragments from the fission of ^{226}Ra by neutrons with $E = 8-10$ MeV were obtained. The neutrons were obtained from the reaction $D(d,n)^3\text{He}$. The deuterons were accelerated to an energy of 6.7 MeV on the cyclotron of the Radium Institute and moderated with platinum foils. The radium fission fragments were recorded by means of mica detectors processed in the usual way [2] after irradiation. The radium target weighing 220 ± 7 μg was obtained by evaporating RaCl_2 in a vacuum onto a nickel backing with a thickness of ~ 500 $\mu\text{g}/\text{cm}^2$. The results of the measurements are given in the table.

Table

Relative differential cross-sections, $\frac{\sigma(\vartheta^{\circ})}{\sigma(90^{\circ})}$, for neutron-induced fission of ^{226}Ra

θ \ E_n (MeV)	$7,9 \pm 0,1$	$9,0 \pm 0,1$	$9,7 \pm 0,1$
11°	$1,30 \pm 0,06$	$1,29 \pm 0,06$	$1,50 \pm 0,06$
21°	$1,36 \pm 0,06$	$1,38 \pm 0,06$	$1,46 \pm 0,06$
34°	$1,27 \pm 0,06$	$1,32 \pm 0,06$	$1,19 \pm 0,06$
47°	$1,11 \pm 0,06$	$1,21 \pm 0,06$	$1,22 \pm 0,06$
61°	$1,20 \pm 0,06$	$1,07 \pm 0,05$	$1,07 \pm 0,05$
76°	$1,01 \pm 0,06$	$1,07 \pm 0,05$	$0,95 \pm 0,05$
90°	$1,00 \pm 0,06$	$1,00 \pm 0,05$	$1,00 \pm 0,05$

The anisotropies were calculated on the basis of these and the earlier measurements [1] of the angular distributions of fragments, which were processed by the method of least squares with expansion in terms of the Legendre polynomials P_0 and P_2 (Fig. 1b). These results were used to calculate the dispersions of the projection of the total angular momentum onto the axis of symmetry of the nucleus at the saddle point, K_0^2 (Fig. 1c). Analysis of the energy dependence and the value of K_0^2 in conjunction with data on the energy dependence of the neutron-induced fission cross-section of ^{226}Ra (Fig. 1a) indicates that the parameter $2\Delta f$ of the energy gap at the saddle point of ^{227}Ra increases to a value of 2.7 ± 0.7 MeV. This value of the parameter $2\Delta f$ can be explained by the significant increase in the surface area of a nucleus at the saddle point in the case of relatively light fissionable nuclei.

REFERENCES

- [1] BABENKO, Yu.A., IPPOLITOV, V.T., NEMILOV, Yu.A., SELITSKY, Yu.A., FUNSHTEIN, V.B., *Jadernaja Fizika* 10 (1969) 233.
- [2] RUMYANTSEV, O.V., SELITSKY, Yu.A., FUNSHTEIN, V.B., *Priboř Tekh. Eksp.* 1 (1968) 51.

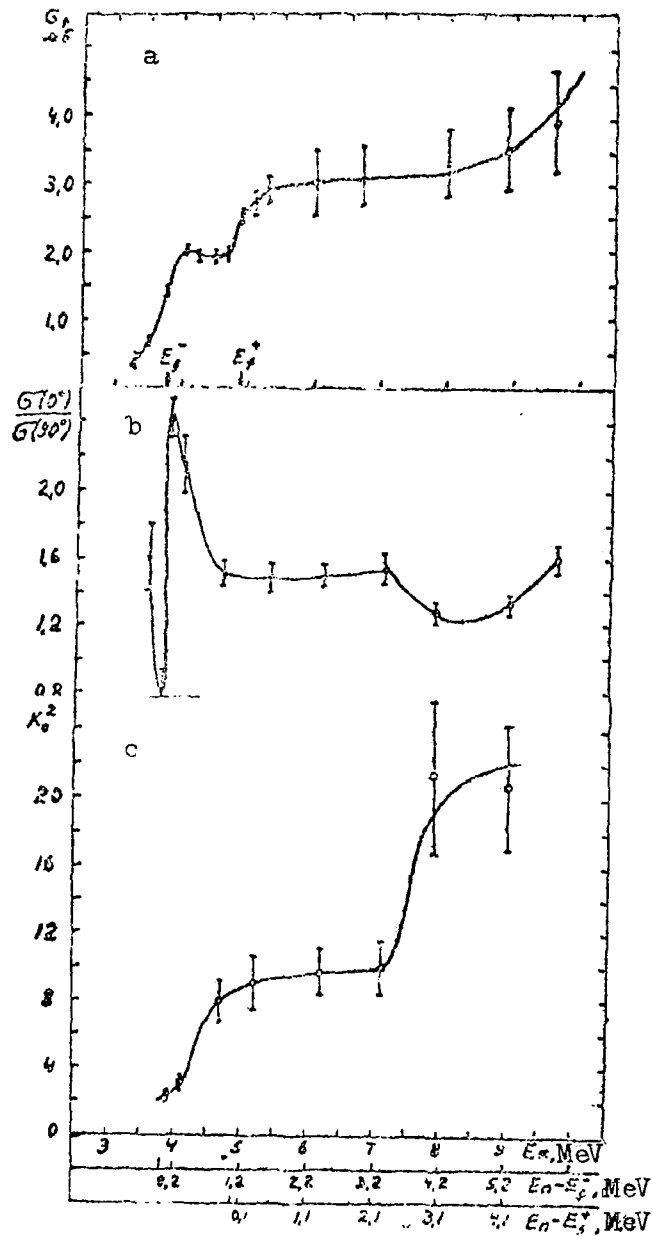


Fig. 1

Neutron energy dependence of: fission cross-section (a), anisotropy of fragment divergence (b) and dispersion in the distribution of the projection of the total angular momentum onto the axis of symmetry of a nucleus at the saddle point (c)

- O = data of this paper
- = data from Ref. [1]

NEUTRON EMISSION ANISOTROPY AND TOTAL KINETIC ENERGY
OF ^{252}Cf FISSION FRAGMENTS

M.V. Blinov, N.M. Kazarinov, I.T. Krisyuk

The authors investigate the dependence of the neutron emission anisotropy A on the total kinetic energy of fragments E_k from spontaneous fission of ^{252}Cf . The relationship $A(E_k)$ was also calculated using the neutron evaporation model. The experimental and theoretical data agree satisfactorily in the region of low E_k and deviate appreciably as E_k increases. This points to the existence of fission neutrons not associated with the evaporation mechanism.

E_k	$A_{\text{exp.}}$	$A_{\text{theor.}}$
153	4,55	4,30
157	4,65	4,75
161	4,27	5,25
165	4,84	5,70
169	5,03	6,15
173	5,10	6,63
177	5,25	7,11
181	5,10	7,54
185	5,36	8,00
189	5,25	7,46
193	5,25	8,40
197	5,18	9,33
201	4,81	9,85
205	4,75	10,3
209	4,66	10,8
213	4,63	-
217	4,25	-

DEPENDENCE OF NUMBER OF NEUTRONS ON ALPHA-PARTICLE
ENERGY IN TERNARY FISSION OF ^{252}Cf

V.A. Adamov, L.V. Drapchinsky, S.S. Kovalenko, K.A. Petrzhak,
L.A. Pleskachevsky, I.I. Tyutyugin

The authors investigate the dependence of the number of neutrons on alpha-particle energy for the angles 0° , 90° and 180° between the directions of movement of an alpha particle and a neutron for ternary spontaneous fission of ^{252}Cf . The alpha particles were recorded with a silicon detector and the neutrons with a stilbene crystal, the signals from neutrons and gamma rays being separated by the shape of the light flash. The experiment showed a difference in the number of neutron-alpha particle coincidences "in" and "against" the direction of movement of the alpha particles. Quantitatively this difference is expressed by the ratio $N_{\text{co"in"}}/N_{\text{co"ag"}} = 1.19 \pm 0.03$, i.e. 19% more neutrons are emitted in the direction of the alpha particles than in the opposite direction. After introducing a correction for the difference in the shape of the spectrum, the angular distribution, the number of neutrons from light and heavy fragments and the effect of the α, n reaction in the detector material the figure is reduced to $17 \pm 3\%$. The alpha particle spectrum for 0° was displaced 3.5 MeV in the direction of lower energies. These data indicate that the asymmetry effect is due to neutron emission by the isotope ^5He or ^6He , since the ^6He spectrum is displaced 4 MeV towards lower energies. The yield of this isotope with respect to the number of coincidences at an angle of 90° is $5.3 \pm 0.9\%$. The data obtained in this study do not allow any conclusions to be drawn as to the preferential yield of ^5He or ^6He .

FINE STRUCTURE IN THE MASS DISTRIBUTION OF FISSION FRAGMENTS

V.A. Korostylev, D.K. Ryazanov, V.A. Safonov

The authors measured the neutron and gamma ray yield for a fine structure in the mass distribution of ^{235}U thermal fission fragments, when the kinetic energy of a light fragment $E_1 = 108.5$ MeV.

The number of neutrons emitted by a heavy fragment was established to be as follows:

For A = 132	$\nu = 0.1 \pm 0.05$
A = 134	$\nu = 0.6 \pm 0.10$
A = 140	$\nu = 0.75 \pm 0.15$
A = 148	$\nu = 1.00 \pm 0.15$
A = 154	$\nu = 1.70 \pm 0.15$

The number of gamma rays does not vary very much with the mass and, on average, is seven rays per fission event.

THE MASS DISTRIBUTION OF LONG-RANGE
PARTICLE FISSION FRAGMENTS

V.G. Bogdanov, V.S. Bychenkov, Z.I. Soloveva,
O.E. Shigaev

To construct the mass distribution of long-range particle fission fragments from the relation $E_{\alpha} m_{\alpha} = K E_m m_r$, it is necessary to know the coefficient K which allows for the alpha-particle recoil effect.

$$K = \left(\frac{\sin \varphi_r}{\sin \varphi_{\alpha}} \right)^2$$

where φ_r and φ_{α} are the angles formed by an alpha particle with a light and a heavy fragment.

The authors derive the values of K for different mass ratios R of fragments from long-range particle fission of ^{235}U by thermal neutrons and of ^{238}U by fast neutrons.

R	No. of cases	φ_{α} deg.	φ_r deg.	\bar{K} averaged
$1,0 < R < 1,3$	150	83,7	101,5	$0,979 \pm 0,008$
$1,3 < R < 1,6$	212	82,4	102,1	$0,973 \pm 0,007$
$1,6 < R < 2,0$	137	80,3	104,6	$0,958 \pm 0,008$
$R \geq 2,0$	45	79,1	107,1	$0,903 \pm 0,030$
Total	544	81,9	102,3	$0,965 \pm 0,004$

SCIENTIFIC RESEARCH INSTITUTE FOR ATOMIC REACTORS

DELAYED NEUTRONS FROM SPONTANEOUS FISSION OF ^{252}Cf

V.N. Nefedov, A.K. Melnikov, B.I. Starostov

In this study experiments were performed to determine the energy, emission time and the number of delayed neutrons emitted during spontaneous fission of ^{252}Cf . The time-of-flight method was used to determine the energy of separate groups of delayed neutrons. The measurements were performed on a path length of 3.5 m. The recorded spectrum clearly showed the separate peaks formed by the delayed neutrons. The peak energies are: 0.5 ± 0.01 MeV, 0.7 ± 0.01 MeV, 1.16 ± 0.02 MeV, 1.6 ± 0.03 MeV, 2.6 ± 0.1 MeV. The delayed neutron emission times have been estimated for certain peaks and these are shown in Table 1.

Table 1

No.	Peak energy MeV	Emission time nsec
1	0.7 ± 0.01	5 - 10
2	1.16 ± 0.02	2 - 3
3	1.6 ± 0.03	5 - 10

The method of delayed coincidences was used to determine the emission times of separate groups of delayed neutrons and their yield. These data are given in Table 2.

Table 2

No.	Emission times of groups of delayed neutrons, T, nsec	Yield of delayed neutrons as % of total number of neutrons per fission
1.	2 ± 0.5	2.7 ± 0.4
2.	7 ± 1	0.6 ± 0.1
3.	30 ± 2	0.11 ± 0.03
4.	80 ± 5	
5.	120 ± 20	

THE D.I. MENDELEEV ALL-UNION INSTITUTE FOR
METROLOGY RESEARCH (VNIIM)

DETERMINATION OF THE INTEGRAL PARAMETERS OF
NEUTRON INTERACTION WITH CARBON

V.T. Shcheboleva

The author describes a method for determining the distance of constant spectral sensitivity in graphite to neutrons emitted by various sources. This was found to be 0.82 m for the VNIIM facility.

The diffusion length in graphite was determined by the "negative" source method, the result being 0.520 ± 0.002 m. The method of comparing the normalized distribution curves of thermal neutrons with the theoretical curves was used to measure the neutron moderation lengths in graphite. The results were 0.2270, 0.2054, 0.2022, 0.1991 and 0.1911 m respectively for the sources $T(d,n)^4\text{He}$, $\text{Pu-Be}(\alpha,n)$, $\text{Ac-Be}(\alpha,n)$ and $\text{PoB}(\alpha,n)$. The maximum error in measuring the age is 0.8%. It was found that the average energy of the $\text{Ac-Be}(\alpha,n)$ source should be taken as 4.1 MeV, i.e. 11% less than that quoted hitherto.

ALL-UNION INSTITUTE OF PHYSICOTECHNICAL AND
RADIOTECHNICAL RESEARCH

APPLICATION OF AN ITERATION METHOD FOR RAPID
CONSTRUCTION OF ARBITRARY SPECTRA

V.S. Troshin, E.A. Kramer-Ageev, R.D. Vasilev, E.I. Grigorev,
G.B. Tarnovsky, V.P. Yaryna

(Article published in the Bulletin, issue No. 7, 1970)

An iteration method is used for constructing a fast neutron spectrum from the results of activation measurements based on effective thresholds and cross-sections. On the basis of data supplied in graph form, a spectrum is constructed without the aid of a computer. The error in the values for the differential neutron flux density is estimated as 15%.